AD-A164 495 INVESTIGATION OF HIGH AND LOW PREDICTABILITY PERIODS IN MEDIUM RANGE FORECASTS(U) NAVAL POSTGRADUATE SCHOOL MONTEREY CA J E CURTIS DEC 85 1/1

UNCLASSIFIED F/G 4/2 NL

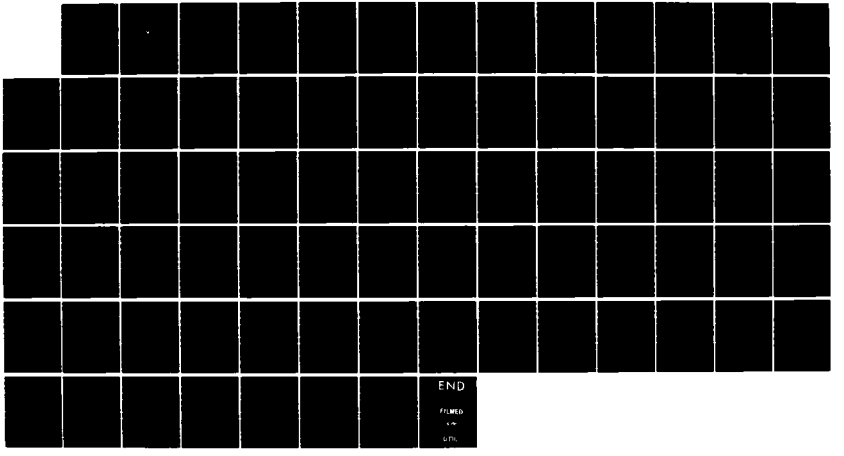

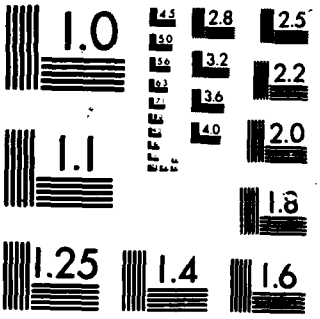

MICROCOPY RESOLUTION TEST CHART

NATIONAL BUREAU OF STANDARDS 1963 A

(2)

NAVAL POSTGRADUATE SCHOOL
Monterey, California

THESIS

INVESTIGATION OF HIGH AND LOW PREDICTABILITY PERIODS IN MEDIUM RANGE FORECASTS

by

John Edward Curtis

December 1985

Thesis Advisor: C.H. Wash
Co-advisor: J.S. Boyle

Approved for public release; distribution is unlimited

UNCLASSIFIED
SECURITY CLASSIFICATION OF THIS PAGE

AD-A164 495

REPORT DOCUMENTATION PAGE

1a. REPORT SECURITY CLASSIFICATION	1b. RESTRICTIVE MARKINGS
2a. SECURITY CLASSIFICATION AUTHORITY	3. DISTRIBUTION / AVAILABILITY OF REPORT Approved for public release; distribution unlimited
2b. DECLASSIFICATION / DOWNGRADING SCHEDULE	
4. PERFORMING ORGANIZATION REPORT NUMBER(S)	5. MONITORING ORGANIZATION REPORT NUMBER(S)
6a. NAME OF PERFORMING ORGANIZATION: Naval Postgraduate School 6b. OFFICE SYMBOL (If applicable): 63	7a. NAME OF MONITORING ORGANIZATION: Naval Postgraduate School
6c. ADDRESS (City, State, and ZIP Code): Monterey, California 93943-5100	7b. ADDRESS (City, State, and ZIP Code): Monterey, California 93943-5100
8a. NAME OF FUNDING / SPONSORING ORGANIZATION 8b. OFFICE SYMBOL (If applicable)	9. PROCUREMENT INSTRUMENT IDENTIFICATION NUMBER
8c. ADDRESS (City, State, and ZIP Code)	10. SOURCE OF FUNDING NUMBERS PROGRAM ELEMENT NO. / PROJECT NO. / TASK NO. / WORK UNIT ACCESSION NO.

11. TITLE (Include Security Classification)
INVESTIGATION OF HIGH AND LOW PREDICTABILITY PERIODS IN MEDIUM RANGE FORECASTS

12. PERSONAL AUTHOR(S)
Curtis, John E.

13a. TYPE OF REPORT	13b. TIME COVERED	14. DATE OF REPORT (Year, Month, Day)	15. PAGE COUNT
Master's Thesis	FROM _____ TO _____	1985 December	75

16. SUPPLEMENTARY NOTATION

17. COSATI CODES			18. SUBJECT TERMS (Continue on reverse if necessary and identify by block number)
FIELD	GROUP	SUB-GROUP	Medium Range, predictability, five day forecasts, NOGAPS, 500 mb height fields, flow characteristics, error persistence

19. ABSTRACT (Continue on reverse if necessary and identify by block number)

Medium-range five-day forecasts from the U.S. Navy Operational Global Atmospheric Prediction System (NOGAPS) are investigated to study high and low predictability periods from two winter seasons. Northern hemisphere 500 mb height fields are scored using the anomaly correlation coefficient. An objective method is used to choose high and low scoring periods which are analyzed using height tendencies and wavenumber structure. Results show that it is possible to objectively determine why some high and low periods occurred. Flow characteristics leading to high scoring five-day forecasts include: long wave amplitude decay, transition from meridional to zonal flow, and more meridionally e extensive flow patterns. This study revealed that persistence is not a good indicator of model performance, and no appreciable skill difference exists between good and poor five-day forecasts at the 48 hour point. However, no single measure of the flow patterns is found to be a unique indicator of high or low scoring forecasts.

20. DISTRIBUTION / AVAILABILITY OF ABSTRACT	21. ABSTRACT SECURITY CLASSIFICATION
☒ UNCLASSIFIED/UNLIMITED ☐ SAME AS RPT. ☐ DTIC USERS	Unclassified
22a. NAME OF RESPONSIBLE INDIVIDUAL: Prof. C.H. Wash	22b. TELEPHONE (Include Area Code): 408-484-2345 / 22c. OFFICE SYMBOL: 63Wa

DD FORM 1473, 84 MAR — 83 APR edition may be used until exhausted. All other editions are obsolete.

SECURITY CLASSIFICATION OF THIS PAGE
UNCLASSIFIED

Approved for public release; distribution is unlimited.

Investigation of High and Low Predictability Periods in Medium Range Forecasts

by

John E. Curtis
Lieutenant, United States Navy
B.S., United States Naval Academy, 1978

Submitted in partial fulfillment of the
requirements for the degree of

MASTER OF SCIENCE METEOROLOGY AND OCEANOGRAPHY

from the

NAVAL POSTGRADUATE SCHOOL
December 1985

Author: John E. Curtis
John E. Curtis

Approved by:
C.H. Wash, Thesis Advisor

J.S. Boyle, Co-Advisor

R.J. Renard, Chairman,
Department of Meteorology

John N. Dyer,
Dean of Science and Engineering

ABSTRACT

Medium-range five-day forecasts from the U.S. Navy Operational Global Atmospheric Prediction System (NOGAPS) are investigated to study high and low predictability periods from two winter seasons. Northern hemisphere 500 mb height fields are scored using the anomaly correlation coefficient. An objective method is used to choose high and low scoring periods which are analyzed using height tendencies and wavenumber structure. Results show that it is possible to objectively determine why some high and low periods occurred. Flow characteristics leading to high scoring five-day forecasts include: long wave amplitude decay, transition from meridional to zonal flow, and more meridionally extensive flow patterns. This study revealed that persistence is not a good indicator of model performance, and no appreciable skill difference exists between good and poor five-day forecasts at the 48 hour point. However, no single measure of the flow patterns is found to be a unique indicator of high or low scoring forecasts.

TABLE OF CONTENTS

LIST OF TABLES

LIST OF FIGURES

ACKNOWLEDGEMENTS

My sincere thanks to Dr. Wash, for his strategic directives and synoptician's eye; to Dr. Boyle for his tactical guidance and superb computer graphics programs which are the heart of this thesis; to my wife Donnarae for her care and understanding; and to GOD, through whom all things are possible.

I. INTRODUCTION

Current numerical weather prediction systems contain errors from various sources; data inaccuracies, initialization, irregular or inadequate distribution of observations, or systematic errors from the model itself (Haltiner and Williams, 1980).

Prediction problems arising from these errors can be divided into three categories, depending on the time scale of the forecast (Grønaas, 1982). The first are the short range forecasts, mainly affected by the initial conditions of the model. The second are the long - term forecasts which are largely independent of the initial data. This includes the problem of the model drifting from the real atmospheric climatology to its own climatology. The third category between these extremes is the medium range forecast. Bengtsson and Simmons (1983) define this time scale as being a few days to a week or two. In this study the medium range forecast category will be defined as four to five days in length.

Medium range forecasting today is in much the same position as short range forecasting was in the in the early days of numerical weather prediction (NWP). Now, as then, one finds that the forecasts have some useful information in them, but they also contain a considerable amount of systematic error (Grønaas, 1982).

Compared to the early NWP models, however, the systematic errors in today's complex NWP models are much less predictable (Grønaas, 1982). The end result is that the meteorologist forecasting in the medium range must use subjective synoptic skills to extract useful information from the weather forecasts or rely on climatology and persistance (usually as a last resort) to sort out the poor from the good forecasts.

It is known that there are times when the medium range forecasts produced by any of the major operational centers are exceptionally accurate, and other times when they are exceptionally poor. For example, time series representations of the Anomaly Correlation Coefficient (ACC) in studies by Grønaas (1982), Bengtsson and Simmons (1983) and Bengtsson (1985) at the European Center for Medium Range Forecasts (ECMWF) have revealed that there are periods when the medium range forecasts have a relatively high ACC score. Assuming that values of this correlation coefficient of 0.5 or 0.6 indicate the limit of usability of a forecast field (e.g., Hollingsworth et al., 1980), these studies show there are periods of time when the 0.7 value is exceeded five days beyond forecast time.

These "Spells of Time when the ACC is Relatively High" (hereafter referred to as a STARH and pronounced 'star') occur without any apparent periodicity and last anywhere from around two to twenty-two days long. Although Bengtsson and Simmons (1983) did not give a reason for STARH existence, they stated that investigating the reason for these spells of high and low predictability is an important research topic. Bengtsson (1985) suggests that these periods might occur because either the model can handle certain situations better than others, or that the accurate periods occur in a regime that is inherently more predictable.

Grønaas (1982) showed subjectively that these periods are to a large extent related to the large scale flow patterns. The STARH occurred when the synoptic wind flow pattern was more meridional in nature, and poor forecast periods occurred during times when zonal flow dominated. Nieminen (1983) also indicates that the ECMWF model has indications of being more skillful in periods of more meridional flow, for example, in blocking regimes.

Bettge and Baumhefner (1984) conclude in their study of the FGGE data that model forecast skill was strongly influenced by the planetary wave structure. The long-term oscillations in the forecast skill were found to be related to rapid transitions in the planetary waves; good predictions occurred when the waves were relatively stationary (blocking situations) and poor forecasts were found during the transition periods. These poor predictions, or "Forecasts of Low Predictability" are hereafter referred to as FLOPs.

This information suggests that it might be possible to objectively quantify parameters of the atmospheric flow patterns that would explain the cause of these high and low predictability periods in medium range forecasts. It is interesting to note that Elsberry, et al. (1985) indicate that there has been no method developed or tested to determine the accuracy of a medium range forecast based on the day one forecast error. Also, Bengtsson (1985) stated that the cause of high and low predictability periods is a fundamental question to which no conclusive answer can yet be given.

The objectives of this study, then, are twofold. First, to develop a method to objectively choose high (STARH) and low (FLOP) predictability periods. Second, to investigate the flow patterns of the chosen periods and study the effect on the forecast score of the following:

- Persistence
- Early error growth
- Error pattern locations
- Average height field tendencies and standard deviation differences
- Zonal wavenumber structure
- Meridional wavenumber structure

Chapter two of this study discusses the the source of the data used in this investigation and the method employed to score the forecasts. Chapter three details the objective method for choosing STARH and FLOP periods and a summary of

the periods selected. Chapter four presents the analysis methods employed to investigate the good and bad forecast periods and a summary of the number of periods accounted for by each analysis method. The conclusions and recommendations for future research are summarized in Chapter five.

II. DATA SUMMARY AND SCORING METHOD EMPLOYED

A. DATA SUMMARY

Medium range forecasts produced by NOGAPS (Navy Operational Global Atmospheric Prediction System) are studied in this thesis. The data was retrieved from the Model Output Statistics data base stored at the Fleet Numerical Oceanography Center (FNOC) in Monterey, California.

NOGAPS is a nine layer gridpoint model with a horizontal resolution of 2.4° latitude by 3.0° longitude. The maximum NOGAPS forecast length is five days, generated once a day from the 0000 GMT analysis data. This limits the study to five-day forecasts.

The current version of NOGAPS, 2.1, was implemented on 8 December 1983. Since that time, an error in the latent heating term was detected (it was one half the correct value). This error was corrected in April 1984.

Only the northern hemisphereic section of the global data base was investigated. This is because forecast accuracy and usefulness is substantially less in the southern hemisphere due to a sparsity of data. This was demonstrated to be the case for the ECMWF model by Bengtsson and Simmons (1983), and was also found to be true of the NOGAPS model in preliminary investigations of this study.

The winter season forecasts were used for the investigation of the high and low predictability periods, since winter is the season with the largest number and the most energetic systems. Also, it is recognized that model ACC scores tend to be higher in winter than in summer.

There were only two winter seasons of data available since the NOGAPS 2.1 model became operational on 8 December 1983. The total number of days possible to use in this study were 83 days from the 1983 winter season (8 December

1983 - 29 February 1984) and 90 days from the 1984 winter season (1 December 1984 - 28 February 1985). The actual number of days available for use in this study was a few days less than the total possible due to missing model runs or other related problems. For the 1983 winter season, 80 of 83 five-day forecasts (0.964 percent) and for the 1984 winter season 82 of 90 five day forecasts (0.911 percent) were available.

Time constraints limited this study to investigating only one level of the atmosphere. The 500 mb level was used since it is the most accurately forecasted level in the medium range. Also, several other authors (i.e., Hollingsworth et al., 1980, Wallace and Woessner, 1983, Grønaas, 1982, Bettge, 1983, Bengtsson and Simmons, 1983, Bettge and Baumhefner, 1984, and Bengtsson, 1985) have used the 500 mb height field (alone or in conjunction with the other height fields) when scoring model forecasts or describing the state of the atmosphere. Investigating this level allows for comparability between this and other studies.

B. SCORING TECHNIQUE

The anomaly correlation coefficient (ACC) is used for scoring forecasts in this study following Hollingsworth, et al., (1980). It is defined as the correlation between the observed and predicted deviations from climatology, as used by Miyakoda et al. (1972) in their study of medium range forecast predictability.

Grønaas (1982) states that the ACC is probably the best single scoring technique available when used with care, and he notes that there is a correlation between the ACC and the standard deviation of the height errors. He also points out that the ACC is not the ideal scoring method. It is sensitive to phase errors and often mesoscale features score low due to errors in the system's propagation speed. Also, subjectively graded forecasts may score high even when the

ACC produced is low. For example, a forecast poor in synoptic detail or timing may score badly while still giving some indication of an overall change in the weather type (Bengtsson and Simmons, 1983).

Following Miyakoda (1972), the ACC is defined to be:

$$ACC = \frac{\Sigma (F-C)*(O-C)}{\sqrt{(\Sigma(F-C)^2 * \Sigma(O-C)^2)}} \qquad (2.1)$$

where: F = Forecast parameter
O = Observed value
C = Climatology value

Since the climatology data base was not available from FNOC, a monthly mean 500 mb height was used for climatology.

A further qualification was made as to the latitudes over which the ACC was calculated, following Bengtsson and Simmons (1983). Only those grid points within the latitude band 20° to 82.5° were included in the calculation to avoid the tropics and the polar region. This is done because all present day NWP models are poor in the tropics and finite differencing type models require special handling at the poles (Haltiner and Williams, 1980).

III. DISCUSSION OF SELECTED PERIODS

A. OBJECTIVE DEFINITION OF PREDICTABILITY

An objective measure of what constitutes a high or low predictability period in a numerical weather prediction forecast is desired. Hollingsworth et al. (1980), states that an anomaly correlation coefficient value of 0.5 or 0.6 is the limit of useful predictability.

Grønaas (1982) divides the high versus low predictability forecasts by comparing the average 3-, 5-, and 7-day ACC values for a period of interest (the periods being from 3 to 26 days long) to the same for the yearly averaged values, and he subjectively decides if each one is a high or low predictability period.

This study will only examine the most significant periods of the five-day forecasts that were well or poorly forecasted. To this end the high and low predictability periods are chosen as follows:

- The ACC is calculated in the latitude band from 20° to 82.5° N for the entire winter.
- The good periods are initially determined by those periods where the ACC is above 0.6 (the limit of useful skill), and the poorly forecasted periods being those below 0.4 (to limit the data set to the very worst cases).
- The ACC for these periods are averaged, and compared to the mean and standard deviation of the ACC for the entire winter data set.
- If the average ACC for the period is one or more standard deviations above or below the long term mean, the period is accepted as either a STARH (high score) or a FLOP (low score).

B. SUMMARY OF SELECTED PERIODS

Figs. A.1 and A.2 show the time series of the anomaly correlation coefficient plotted as a function of the day (solid line) for both winter data sets. The convention adopted for these graphs is that the score listed above a day is the ACC score of the five-day forecast that was

generated on that day (and whose verification time was 120 h later). Also shown on these figures is the persistence ACC score, plotted as a function of the day (dashed line). This score, computed as was the five-day forecast ACC, uses the analysis field as the five-day forecast.

Table 1 is a summary of the STARH and FLOP periods selected. The statistics listed in Table 1 show each period meets the selection criterion established in the previous section. Shown are the thirteen selected periods, consisting of six STARH and seven FLOP periods evenly divided between the two winters. The rationale for the numbers assigned to the periods is that the one-digit numbers are periods from the 1983-84 winter season, while the two-digit numbers refer to periods from the 1984-85 season. Winter 1983-84 periods are not consecutively numbered because other periods had been initially selected but were later discarded when the selection criterion was imposed.

The period of time over which the STARHs or FLOPs exist varies from the shortest of two days (periods S5, F4, and S12) to the longest of twelve days (period S10). It is also interesting to note that like periods do not all occur in the same month or in a close period of time, but exist in more of a random distribution pattern.

These selected periods are now studied in detail to better understand the reasons for such variation in medium-range forecast performance.

IV. INVESTIGATIONS ON MEDIUM RANGE FORECASTING

The flow patterns of the chosen periods are studied in order to quantify the forecast score variance due to persistence, early error growth, error pattern locations, average height field tendencies, standard deviation differences, zonal wavenumber structure and meridional wavenumber structure.

A. THE ROLE OF PERSISTENCE

Persistence of the atmospheric flow patterns is naturally a candidate to explain the existence of high and low predictability periods. If persistence is a strong factor, one would expect that a flow pattern that exhibited little change through the forecast period would verify with a high score, while periods of strong flow pattern change would verify poorly.

Figs. A.1 and A.2 show the persistence score as a function or forecast day. Examining these figures for the STARH and FLOP periods, one sees that persistence is a poor indicator of model performance. For example, Fig. A.1 shows persistence ACC score to peak at the same time as STARH S1 (26-30 December 1983), but it also peaks at the same time as FLOPs F1 (30-31 January 1984) and F8 (15-21 February 1984).

The number of selected periods explained well or poorly by the persistence method is listed in Table 2 One finds that five periods can be accounted for by the persistence method (S1, F4, F7, S11, and F12), but six others (S2, S5, F1, F8, S12, and F11) are periods where the persistence value is just opposite to what would be expected using this analysis method. It is evident that with as many periods occurring oppcsite of what is expected in both winters and

for both STARHs and FLOPs, persistence is not a good indicator of model forecast score in the medium-range.

Additional tests were run on the correlation between the model forecast ACC time series curve and the persistence ACC curve of Figs. A.1 and A.2 The results are shown in Table 3 for winter 1983-84 and in Table 4 for winter 1984-85. If persistence was to be a good indicator of the forecast ACC, the correlation between the model and persistence forecast ACC curves would be high (close to one). Any correlation would produce a value at least above zero. It can be seen in these tables that only for one month (December 1983) is the persistence ACC curve highly correlated with the forecast ACC curve (correlation value of 0.47). This correlation is also evident on Fig. A.1 Three of the months show negative correlation values (January and February 1984, and February 1985), while the other two months have small positive values.

It is interesting, that in one month (December 1983) of the six months studied, the medium-range forecast score variance was so highly correlated with persistence. Quiroz (1984) states that December 1983 was a month of unusually strong blocking patterns over North America. This may, in part, explain why the December ACC score so strongly paralleled the persistance score.

In any case, the fact that persistence is not a good indicator of forecast skill in this data set is consistent with the results of Bengtsson and Simmons (1983) who also found high medium-range forecast scores in times when a large changes occurred in the height fields through the forecast period.

B. THE ROLE OF EARLY ERROR GROWTH

More data available for a NWP model initialization should lead to better short and medium-range forecasts. This suggests that one reason for poor model performance in the medium-range might be the quality or quantity of the

initial data. If model skill is affected by these errors in the initial data field, one would expect to see a lower ACC score immediately in the forecast period for the FLOP periods, and a higher ACC score in this same period for the STARHs.

The average ACC values of each selected period as a function of time are presented in Figs. A.3, A.4, A.5, and A.6 . These figures show the trend of the average forecast score for each period over the five-day forecast period. Comparing the STARH periods of winter 83-84 on Fig. A.3 to the FLOPs of that winter on Fig. A.4, little difference between the STARHs and FLOPs is present out to 48 hours. Only one FLOP, F8, is seen to have a noticeably lower ACC at the 48-hour point. F4 and F7, however, cannot be distinguished from the STARHs at this time, and F1 is only slightly lower than the the lowest scoring STARH at 48 hours (S2).

It is interesting to note that F8, although scoring much lower than the other FLOPs at 24, 48 and 72 hours, is at almost the same ACC value at 96 and 120 hours. This indicates that early errors for F8 did not produce a 120-hour ACC score significantly below the other FLOPs.

Comparing the STARHs and FLOPs from winter 84-85 on Figs. A.5 and A.6 shows similar results. At 48 hours the ACC of the STARHs are all higher than the FLOPs, but the STARHs and FLOPs are very close on the ACC scale. They are all within 0.05 of each other, and the highest FLOP is only about 0.02 below the lowest STARH. Although there are not enough data to assign a statistical significance to this grouping of points, it is clear that for both winters the largest difference in ACC between the STARH and FLOP periods lies at the 72-hour point and beyond. In the summary of results (Table 2) only one of the 13 periods (F8) shows an

expected result. The rest show no indication that early error growth was an indicator of the five-day ACC scores.

The obvious conclusion is that the errors present early in the forecast period of the FLOP periods are not significantly different from those present in the STARH periods, and that initial data errors, as revealed by the ACC scoring method, do not seem to play a major role in determining forecast skill in the medium-range. This result is dependent upon our choice of scoring the forecasts. Other medium-range skill scores may be more sensitive to early errors.

C. THE ROLE OF ERROR PATTERNS

1. Summary of Error Sources for the STARH and FLOP Periods

This section summarizes the features in the analysis charts of the 500 mb height field that differed from the forecasted height field for all the good and poor forecast periods. By comparing the error patterns (generated by the subtracting the 500 mb verifying day analysis from the 500 mb five-day forecast) to the verifying day analysis, one could identify the flow pattern features related to the error patterns. Retracing in time the evolution of the feature, it was possible to gain some insight as to why some periods scored poorly and why others scored rather well.

Examining all the selected periods in the winter season 1983-84 in this fashion revealed that the major sources of errors in the forecast field could be reduced to a few features in common to all the periods. While the basic cause of the errors was found to be the same for both the STARHs and FLOPs, it should understood that the sizes and amplitudes of systems causing the error patterns in the STARHs were much smaller. The most common features that caused the large error patterns are listed below:

- Formation of a major ridge late in the forecast period (around day three to day five).
- The formation of a major trough late in the forecast

period (around day three to day five).

- The rapid deepening of a low pressure center or development of a shortwave trough within days three to five of the forecast period.
- The formation of a cutoff low pressure center after day two of the forecast period.
- The regression of a low or high pressure center after day two of the forecast period.
- Inability to maintain the intensity of major high or low pressure centers that persist throughout the forecast period.

These features were almost always under forecasted by NOGAPS. That is, the highs were too low and the lows were too high in the five-day forecast. There were instances in which the sense of the error was just the opposite as this, but these cases were by far fewer and accounted for a only a small part of the total error field.

It is interesting to note that in the summary of the errors listed previously, most of the error causing systems were ones that developed after day two in the forecast period. This corresponds with Figs. A.3 through A.6 which show the largest difference in ACC scores between the STARH and FLOP periods is after day two as well.

2. Geographic Location of Errors

An example of the types of errors encountered is shown on Figs. A.7 through A.11 . Fig. A.7 is a northern hemisphere polar stereographic (PS) 500 mb height analysis from 23 December 1983. The five-day forecast made from this analysis was a FLOP (F4) and verified against the 500 mb height field analysis of 28 December 1983, shown in Fig. A.9 The forecast errors (forecast minus observed height values) are shown on Fig. A.8, with contour intervals of 160 meters. Comparing this with Fig. A.9 one can quickly discern that the largest area and amplitude errors are associated with features that intensified or developed within the forecast period. The most noticeable features on Fig. A.9 associated with large error patterns are the omega block over western Europe, the family of lows across the North Pacific Ocean,

the ridge along the west coast of North America, and the trough over north central Canada (the area around Baffin Island).

The five-day forecast generated from the 28 December analysis was a STARH, and verified against the analysis of 02 January 1984, shown on Fig. A.11 The plot of the error patterns for this forecast, similar to Fig. A.8, is shown on Fig. A.10 Not surprisingly, the size of and number of the error patterns greater that 160 meters is much smaller, indicating the forecast field captured most of the changes that had occurred.

The features on Fig. A.11 that correspond to the error patterns of Fig. A.10 are not nearly as spectacular as they were for Fig. A.8 Two of the error patterns (over England and in the mid-Pacific Ocean) are associated with mostly zonal flow,while two others (Greenland-Newfoundland area and the Black Sea region) are associated with short wave troughs. The remaining error pattern is related to a diffluent trough along the west coast of North America.

In looking at all the error pattern maps for all the STARH and FLOP periods of the 83-84 winter, it was evident that most of the differences in error patterns between the STARH and FLOP periods are within the latitude band of roughly 30° to 60°. Both STARH and FLOP periods were seen to have large errors north of 60° north latitude, but not too surprisingly, only the FLOP periods had large area and amplitude errors in several locations within the 30° to 60° latitude band.

Both STARHs and FLOPs had errors caused mostly by systems that developed late in the forecast period (after day two). The FLOP periods had large scale development of systems roughly within this latitude band over the forecast period, while the STARHs did not show this feature. To determine if these developing large amplitude error patterns were occurring systematically in the same geographic loca-

tions, the error patterns were averaged within the latitude band 30° to 60°, and each day's values were plotted as a function of longitude in a Hovmüller diagram shown on Fig. A.12 for winter 1983-84, and Fig. A.13 for winter 1984-85.

These two figures show the mean error at each longitude through time, with time increasing to the top of the graph. Negative values of the forecast minus observed field are shown as dashed lines.

Cross referencing the days when the FLOPs occurred with the longitude of the large error areas shows that for both winters no one longitude has positive or negative errors that uniquely define FLOPs. The error patterns have rather a random appearance to them without much longitudinal alignment.

It is well known that certain areas of the world experience more frequent cyclogenesis than others (lee of major mountain ranges, east coasts of continents, etc.,). What Figs. A.12 and A.13 indicate is that the FLOPs are associated with large scale development (not just cyclogenesis) almost anywhere within the latitude band 30° to 60° N. Apparently, no one area (longitude) is preferred over another in the generation of a poor forecast.

D. ROLE OF HEIGHT CHANGES

Blocking situations have been attributed to high predictability periods by some authors in past literature (Grønaas, 1982, and Bettge and Baumhefner, 1984). Fig. A.9, the analysis height field for 28 December 1983 (discussed earlier), shows such a case. Here, the 500 mb flow pattern is in a low index state (strong meridional flow) with a classic omega block over western Europe and a simple block over the Gulf of Alaska.

It was stated earlier that the main difference between the STARH and FLOP periods is the lack of development of systems over the five-day forecast time for the STARHs. The analysis charts from 28 December 1983 (Fig. A.9) to the

verifying day of 02 January 1984 (Fig. A.11) and the error pattern associated with the five-day forecast (Fig. A.10) presents an excellent example of this difference. The large blocking systems of 28 December decayed and were minimal sources of error while no new systems developed.

The tendency of the STARH periods to exhibit less development and more of a decay of the existing high amplitude systems can be described as the flow shifting from a low to a high index regime (meridional flow to zonal flow transition). The opposite would then apply to the FLOPs.

NOGAPS systematic errors at 500 mb (Boyle and Wash, 1985) are to fill troughs and weaken ridges. Thus, NOGAPS will verify better in the medium-range when the atmosphere trend (relaxing of high amplitude systems) follows the model systematic error trend.

To objectively quantify this flow pattern behavior, the 500 mb analysis height fields were averaged between 30° and 60° N latitude (the latitude band in which it appeared the STARHs had less errors and the FLOPs had more errors). Each day's average values were plotted as a function of longitude in a Hovmüller diagram as shown in Figs. A.14 and A.15 . The zonal mean is removed so the low height areas show dashed lines, the heavy line is the zero contour, and the high height areas show as solid lines. The heights were contoured at an interval of 80 meters.

These diagrams show the height field anomaly at each longitude for each day. Time increases towards the top of the graph, which allows one to discern how the anomalies (the highs and lows) change over time with respect to any one location. The figures show the typical features of the winter 500 mb patterns, the long wave troughs at longitudes 150°E and 70°W, with ridges at 70°E, 130°W and 20°W.

If the proposed mechanisms are correct, one would expect that as you move forward in time in a STARH period from the day a forecast was generated to its verifying time, the highs would be decaying and the lows would be filling. It is pleasing to note that this is exactly what is seen for some of the periods. In Fig. A.14 , for winter 1983-84, this is the case for periods S1 and S5. By examining the height field for a day in these periods, and then glancing forward in time (towards the top of the figure), one can see that over the five-day forecast period, the lows are filling and the highs are decaying for the most part. The same is true of periods S10 (the last half), and S12 on Fig. A.15 . The shifts in height anomalies expected for the FLOP periods are just the opposite as those for a STARH (i.e., the lows should deepen and the highs should build over the forecast period). This can be seen for F4 and F7 in Fig. A.14 and for F10, F11 and F12 on Fig. A.15

Unfortunately, the height anomaly trend for each type of period does not always occur as expected. The first part of S10 on Fig. A.15 is the best counter example. The highs are building and the lows are deepening, but the model scored high using the ACC (this is certainly what the numerical modelers like to see). These are periods when the model can successfully predict wave amplification in the medium-range. Also, using shifts in height anomalies over time as a method of determining model performance for the medium-range forecasts does not uniquely define STARH and FLOP periods. There are several periods that show the tendencies for a STARH (FLOP) period, yet did not score significantly high (low) with the ACC. For example, on Fig. A.14 one such STARH-like period is from about 8 to 10 February 1984, and a FLOP-like period is around 2 to 3 January 1984. This means that although the technique works for many of the STARHs and FLOPs, it is not unique solely to those periods.

To better illustrate the shifts in the height anomalies over time, the standard deviation of the mean height is calculated for the height field represented on Figs. A.14 and A.15 . The standard deviation of each day's height field is shown on Fig. A.16 for winter 83-84 and Fig. A.17 for winter 84-85.

It is expected that a low index period would have a large standard deviation, as compared to a high index period where a smaller standard deviation value would be calculated. Detecting the change in the standard deviation value over the five-day forecast period is simplified by using Figs. A.18 and A.19 (standard deviation difference graphs for 83-84 and 84-85). This graph is constructed by subtracting the standard deviation of the day at the verifying time from the value at the analysis time. The difference is plotted as a function of time when the five-day forecast was generated.

It is expected that the STARHs would be indicated as positive peaks (showing a tendency of moving from a low to a high index regime) and FLOPS as negative minima. This analysis technique has some successes and some interesting results (results occurring opposite to expectations are termed "interesting" vice "bad" or "failures"). For example, in Fig. A.19 (winter 1984-85), the two largest positive peaks precisely define two STARH periods (S12 and S10, as indicated). Analogously, F10 (a FLOP) is precisely defined as a large "valley" in the negative portion of the graph as expected. This indicates that the shift in height anomalies detected on Figs. A.14 and A.15 can be objectively quantified and is successful in describing some periods.

The other three periods of this winter, however, are not quite as successful. The standard deviation difference for STARH (S11) is generally positive, but not exceptional (the

period 21-25 December which did not have a spectacularly high or low ACC was generally more positive than the period 27-31 December of S11). Similarly, the standard deviation differences of periods F11 and F12 are both mostly negative (as expected), but they are not within distinctly low negative areas (the period 9-12 February is a distinct minimum, but is not a STARH or a FLOP according to the ACC scores).

The most interesting part of Fig. A.19 is the first part of S10 that lies in a large negative portion of the graph (22-29 January). This region has every indication of being a poorly predicted period, yet the model forecasted the changes that occurred very well.

The successes are fewer for the 1983-84 winter period (Fig. A.18). For example, S5 and S1 are within positive peaks of the graph, but other areas of higher positive values exist (15-16 December, 6-10 January, and 17-18 January) that were not spectacularly high or low ACC periods. Also, the FLOPs F1, F4, and F7 do not lie exactly in a local minimum portion of the graph. Nevertheless, these FLOPs are almost all on the negative side of the graph. Neither does STARH S2 lie in a peak of the standard deviation values, and the last day of the period (21 January 1984) is in the negative portion of the graph.

The two most interesting features of this winter are that the large minimum at 22-23 January does not delineate a FLOP, and that F8 has standard deviation differences entirely on the positive side of the graph. This means that the model did poorly even though the flow regime was changing to a more zonal flow pattern (expected to produce good forecasts).

For both winters, these graphs also serve to show periods when the ACC was neither spectacularly high or low, yet look like STARHs or FLOPs because of the large positive

or negative standard deviation differences. This more clearly illustrates that this height anomaly tendency is not a unique indicator of a STARH or FLOP period.

The summary of which periods were not described well by this method is shown on Table 2 In all, four periods had expected results (S1, S5, S12, and F 10), one had results opposite to expectations (F8), and the remaining eight periods had results that were generally as expected, but were either not spectacular or had one or more forecasts in the period that did not fit the hypothesis.

E. ZONAL WAVENUMBER STRUCTURE

Bettge and Baumhefner (1984) used zonal wavenumbers one and two in describing the systematic errors in NMC (National Meteorological Center) forecasts. They conclude that the power (amplitude) distribution in the wavenumbers has a bearing on the predictability of a forecast, such that when the long waves were stationary the medium-range forecast was good. However, when the long waves were in transition, the medium-range forecast was poor.

This technique can also indicate the flow characteristics of a height field. Meridional flow is related to high power (amplitude) in the lower wavenumbers (waves 1-3), while zonal flow is more a function of the power in the higher wavenumbers (4-6).

To investigate how the zonal wavenumber structure of the height fields is related to medium-range predictability, the Fourier decomposition method is used to determine the wavenumber versus amplitude spectrum of each 500 mb analysis height field. The standard fast Fourier transform method was employed (IMSL, 1982). The 500 mb analysis field height anomalies in Figs. A.14 and A.15 were used as the input waveform for the Fourier decomposition routine. The amplitudes (in meters) for each day are plotted as a function of the wavenumber in Figs. A.20 (winter 83-84) and A.21 (winter

84-85). As in the previous Hovmüller diagrams, time is increasing towards the top.

No one "signature" of a denoted STARH or FLOP period is common to both winters in this harmonic analysis. For the 1983-84 winter season, the most characteristic feature of the STARHs is the peak in wave number three (often associated with a blocking situation as in Fig. A.9) and relatively lower amplitudes in waves two and four. However, this characterization of the wavenumber structure of STARHs and FLOPs in the 83-84 winter is not unique to these periods alone. For example, Fig. A.20 shows that there are peaks in wave three on 7 and 17 January 1984 and on 9 February, yet these are not STARHs. Similarly, 20 December 1983 and 14 February have distinct minimums in wave three, yet lie outside of the FLOP periods.

There is no correspondingly high amplitude in wave number three for all the STARH periods of winter 84-85 (Fig. A.21). No conclusion can be drawn about a characteristic structure that would indicate a STARH or a FLOP period since the data set is too small considering the variances encountered within the wavenumber amplitudes.

The indication, discussed earlier, of STARHs to exist when the flow pattern shifts from a meridional to a zonal pattern can also be detected as a shift in the amplitude of the zonal wavenumbers from the analysis amplitude spectrum to that of the verifying amplitude spectrum.

To facilitate detecting these shifts in the amplitude of the major wavenumbers for both winters, a Hovmüller diagram has been constructed that shows the change in amplitude over the five-day forecast period for each wavenumber. Fig. A.22 graphs the five-day tendency of the wavenumbers in winter 1983-84, and Fig. A.23 is the same for winter 1984-85. The tendencies are calculated by subtracting, for each wavenumber, the day one value from the day five value.

Positive values reflect growth in a wavenumber, and negative values reflect decay. The convention for these diagrams is that the difference is plotted as a function of day one and (as before) time increases as one moves toward the top of the diagram.

It is expected that a STARH period will experience a decrease in amplitude in the longer waves and possibly an increase in power in the higher wavenumbers. A shift in amplitude in this sense would be an indication that the flow pattern is shifting from a low index (meridional flow) to a high index (zonal flow) regime. FLOPs would be expected to reflect just the opposite behavior.

This analysis technique meets with more success than did the standard deviation differences technique, as more periods are explained by this method. Table 2 lists seven of 13 periods that have shifts in wavenumber amplitudes as expected (S2, F1, F4, S11, S12, F11 and F12), while the standard deviation method can only account for four of the 13 periods. On the other hand, period F8 shows a tendency that is just the opposite to what is expected. This period also showed a similar result for the standard deviation method. The remaining five periods show show some of the expected shifts in zonal wavenumber amplitude, but also some complex behavior not anticipated. For example, in Fig. A.22, STARH S1 does show a decrease in amplitude at the beginning of the period (26 December) in wave two, but wave one increases though most of the period. On 27 December wave three shows decay, and wave five growth (as expected), but a shift occurs on 29 December when wave one begins to decay and wave two shows growth. Waves four and five (as expected) show growth from then until the end of the period.

Other periods like this are S5 and F7. In the second winter (Fig. A.23) the periods showing expected shifts in wavenumber amplitudes are S11, S12, and F11. Those showing more complex behavior are S10, F10 and F12.

Unfortunately, the data set for these two winters is too small to be able to statistically show that one pattern of behavior in the complex cases is significant, but it is clear that many periods are explained very well by this technique. Most interesting is period F8 which (as it did in the standard deviation difference results) shows results just the opposite to what was expected (i.e., the long waves gained power, while wave four and six lost power over the forecast period). Also intriguing are those periods not scored high or low with the ACC, yet exhibit the same tendencies as a STARH or a FLOP (such as 15-17 December 1984: FLOP-like shift in the wavenumbers, and 15-17 January 1984: STARH-like wavenumber shift). This means that the results so far, though promising, are still not unique to the STARHs and FLOPs.

F. MERIDIONAL WAVENUMBER STRUCTURE

The meridional structure of the flow patterns may be an important factor in determining model performance. Investigation of the north-south extent of the various zonal wavenumbers is the subject of this final section.

It is possible to depict the meridional structure of the flow pattern of an analysis field by examining the meridional wavenumber spectrum. This spectrum can be calculated by using a spherical harmonics decomposition of the 500 mb height field.

The spherical harmonics decomposition of the wave field depicts the amplitude of wavenumbers in two dimensions, zonal and meridional. In this study the spherical harmonics decomposition was conducted using a triangular truncation at N=33 ("N" being the zonal wavenumber) (Haltiner and Williams, 1980).

The wave numbers in the meridional direction are defined in this study as "pole to pole" wavenumbers. In plotting, the amplitude values (in meters) for the pole to pole waves

with the same number of nodes (the same |M-N| wavenumber values, where M is the zonal wave number), were summed and plotted as a function of pole to pole wavenumber.

Several plots of the pole to pole wavenumber structure did not produce any significant results. It was noted, however, in studying the zonal wavenumber structure of the 1983-84 winter season (Fig. A.20) that one difference between the STARH and FLOP periods was a peak in zonal wave three in the STARHs, and a minimum amplitude value in zonal wave three for the FLOPs. To examine the meridional extent of this wave, the analysis height fields of all the days that compose each individual STARH and FLOP period were averaged together to form a representative height field of that period. This height field was used as the input height field for the spherical harmonics decomposition. Fig. A.24 shows the meridional wavenumber structure for zonal wave three of all the STARH periods of winter 83-84 and Fig. A.25 shows the same for the FLOPs in the 1983-84 winter season.

To interpret these diagrams one must recall that a higher amplitude in the lower pole to pole wavenumbers (|M-N| nodes) would indicate less meridional structure, or a more meridional flow component. If the premise is correct that good five-day forecasts are generated on days when the flow patterns are more meridional (low index situation) and the poor forecasts are generated on days when the flow patterns are more zonal (high index situation), then it is expected that the STARHs would show more amplitude in the lower pole to pole wavenumbers, while the FLOPs would be expected to show more amplitude in the higher pole to pole wavenumbers.

In contrasting the amplitude in pole to pole wavenumbers one and four between Figs. A.24 and A.25, the STARH periods have a higher amplitude (more power) in wave one than the

FLOPs. Also, the FLOPs show more amplitude (power) in wave four that do the STARHs. A close inspection of Fig. A.25 shows F8 is an extreme case of having more power in the higher pole to pole wavenumbers. Recall that F8 provided unusual results using the other techniques previously discussed in this chapter.

In summary, all of the STARH and FLOP periods were accounted for in the winter season 1983-84 by this technique. Table 2 shows this result for the STARHs and FLOPs of winter 1983-84 is quite dramatic. This technique works well in delineating the good from the poor medium-range forecasts in this winter.

This same approach, however, does not work well for the STARHs and FLOPs in winter 1984-85. Figs. A.26 and A.27 illustrate the meridional wavenumber structure of zonal wave three for the STARHs and FLOPs of winter 1984-85. The construction and interpretation of these figures is the same as for those of the previous winter (Figs. A.24 and A.25). By contrasting the STARHs on Fig. A.26 to the FLOPs on Fig. A.27, one can detect a slightly lower amplitude in pole to pole wavenumbers three and four of the STARHs as compared to the FLOPs. This is certainly expected, but overall, there is not the strong difference between the periods as in the previous winter. F11 and S11, for example, are not very different from each other, and the peak in wave two of S12 is more suggestive of what is expected from a FLOP period.

The most interesting feature of Fig. A.26 is the period S10. The exceptionally large peak in wavenumber one is typical of the other STARHs. It should be noted that for this analysis technique, only the last half of the days composing S10 were included in the averaging process that produced the average height field to represent S10 (i.e., days 26-31 December were left out). This was done since S10 was a very long period (12 days long) and since it has

already been seen that some other process was occurring at the beginning of this period to cause the ACC score to be large. By isolating the first half of the period it makes more apparent what is happening in the last half of the period S10 to cause the high ACC score. Computation of the meridional wavenumber structure of the entire period, however, showed the graph of S10 to resemble those of S11 and S12.

In general, though, the meridional structure of zonal wave three is not as successful in the winter 1984-85 season. It is apparent from the wavenumber structure of the winter season 1984-85 on Fig. A.21 and for winter 1983-84 on Fig. A.20 that these two winters definitely had a different character. This is emphasised by the strong wave three structure of the STARHs in 1983-84, in agreement with Quiroz (1984) on the description of the 1983-84 winter season.

Quiroz noted that the 1983-84 winter was a season of strong blocking and of intensely cold surface temperatures for North America (setting several low temperature records and qualifying as one of the six coldest winters on record). A quick check of records of the 1984-85 winter reveals that it was not nearly so spectacular a season as the previous winter.

Since these two winters show a marked difference in character, other combinations of wavenumbers were examined for the winter season 1984-85 that might show a difference in character between the STARHs and FLOPs. Extensive experimenting and examining the zonal wavenumber structure of the 1984-85 winter season indicated a difference in the STARHs and FLOPs in the zonal wavenumbers four through six.

Figs. A.28 and A.29 show the meridional wave structure of zonal waves four through six for the STARH and FLOP periods of the 1984-85 winter season. These graphs differ from Figs. A.24 and A.25 only in that the meridional struc-

ture of the combination of zonal waves four through six is depicted.

These two figures (A.28 and A.29) show a clear difference in the shape of the curves for the STARHs and the FLOPs. As expected, the STARHs have a high peak at pole to pole wavenumber one. In general, the FLOPs have a high wave one amplitude as well, but at wave four they clearly have a larger amplitude than do the STARHs. F10 does not have as high an amplitude at wave four as do the other two FLOPs, but it also has a correspondingly lower wave one amplitude.

As seen in Table 2, this technique correctly indicates the expected structure of all the STARHs and FLOPs in the winter season 1984-85. However, examining the structure of the meridional wavenumbers for zonal waves four through six does not provide any differentiation between the STARHs and FLOPs of the previous winters.

G. SUMMARY OF ANALYSIS TECHNIQUES

Table 2 lists for all the periods selected in both winters the ability of the various analysis techniques used in this chapter to describe the features expected to be found in STARHs and FLOPs. A rather simplistic grading scheme is employed to summarize the results of all the techniques. An "X" listed in the row next to a period indicates that the analysis technique listed in the column above the "X" showed expected results. A "/" (slash) denotes some of the days of the period showed expected results or that some of what was expected to be present was present, but not in a spectacular or a unique fashion. A "-" (dash) indicates no clear indication was observed, and an "O" is used when results were obtained that were the opposite of what was expected.

If one analysis technique was to be a perfect indicator of STARHs and FLOPs, one would expect to find nothing but "X's" in the column beneath it. No one technique is perfect

for the STARHs and FLOPs of both winters, but it is interesting to note that between both the standard deviation differences and the Fourier decomposition differences methods only three periods are not fully "as expected". Also interesting is that the Spherical Harmonics method can explain all the periods of one winter if the correct zonal wave or waves are used. Persistence, as discussed earlier, is not a consistent indicator of STARHs and FLOPs. This can be seen as almost an equal mix of "X's" and "O's" appear under that column. Early error growth is also discounted as a means to detect model performance as under the "Early Errors" column dash symbols (indicating no clear indication observed) appear for all periods except F8. This indicates that only in rare occasions does this method apply.

V. CONCLUSIONS AND RECOMMENDATIONS FOR FUTURE RESEARCH

The main conclusion of this study is that it is possible to quantify certain aspects of flow patterns that are indicative of STARH and FLOP periods. These indications include:

- Long wave amplitude decay over the forecast period can lead to a good forecast, while long wave amplitude growth over the forecast period tends to produce poor forecasts.
- Transition of flow pattern from a meridional (low index) to zonal (high index) regime leads to a good forecast period. The opposite case leads to a poor forecast period.
- STARHs are related to periods with less meridional structure (more power in the low meridional wave numbers) while FLOPs are related to periods with more meridional structure.

None of these indications, however, show a unique or overwhelming result. Periods do exist for each of these indicators that fit the criterion, but do not score overwhelmingly high or low using the ACC. Also, some periods that score exceptionally high or low have flow indications (as listed above) that are just opposite to what was expected (i.e., a STARH had flow characteristics indicative of a FLOP and vice versa).

There is more confidence placed in the conclusions that the variance in the ACC was <u>not</u> due to the following:

- Persistence as a good indicator of model performance.
- Early error growth in FLOP periods due to low data availability or some critical data missing.
- Errors consistently occurring in the same geographical area causing FLOPs.

Additionally, the data base available for this study was inadequate to provide a statistically significant basis for determining confidence levels of the listed indications.

Based on the findings of this study, several recommended future research efforts are delineated here that will hope-

fully further our understanding of high and low predictability periods in medium range forecasts.

First, it is recommended to investigate the STARH and FLOP periods in more detail to determine why certain analysis methods used in this study were successful in explaining the existence of some high and low predictability periods but not for others.

A second recommendation is to continue computing ACCs of NOGAPS 5 day forecasts to build up a more significant data base for statistical verification purposes. Expanding the seasons examined will also add to the statistical data base, but will also indicate wether or not the mechanisms that cause STARHs and FLOPs in these other seasons are the same as the ones for the winter seasons.

Third, it is recommended to calculate the ACC for the five-day forecasts at additional levels in the atmosphere to allow other flow patterns to be investigated. The final recommendation is to investigate the possibility that some combination of the parameters measured in these analysis techniques might provide an indication of the potential predictability of a medium range forecast.

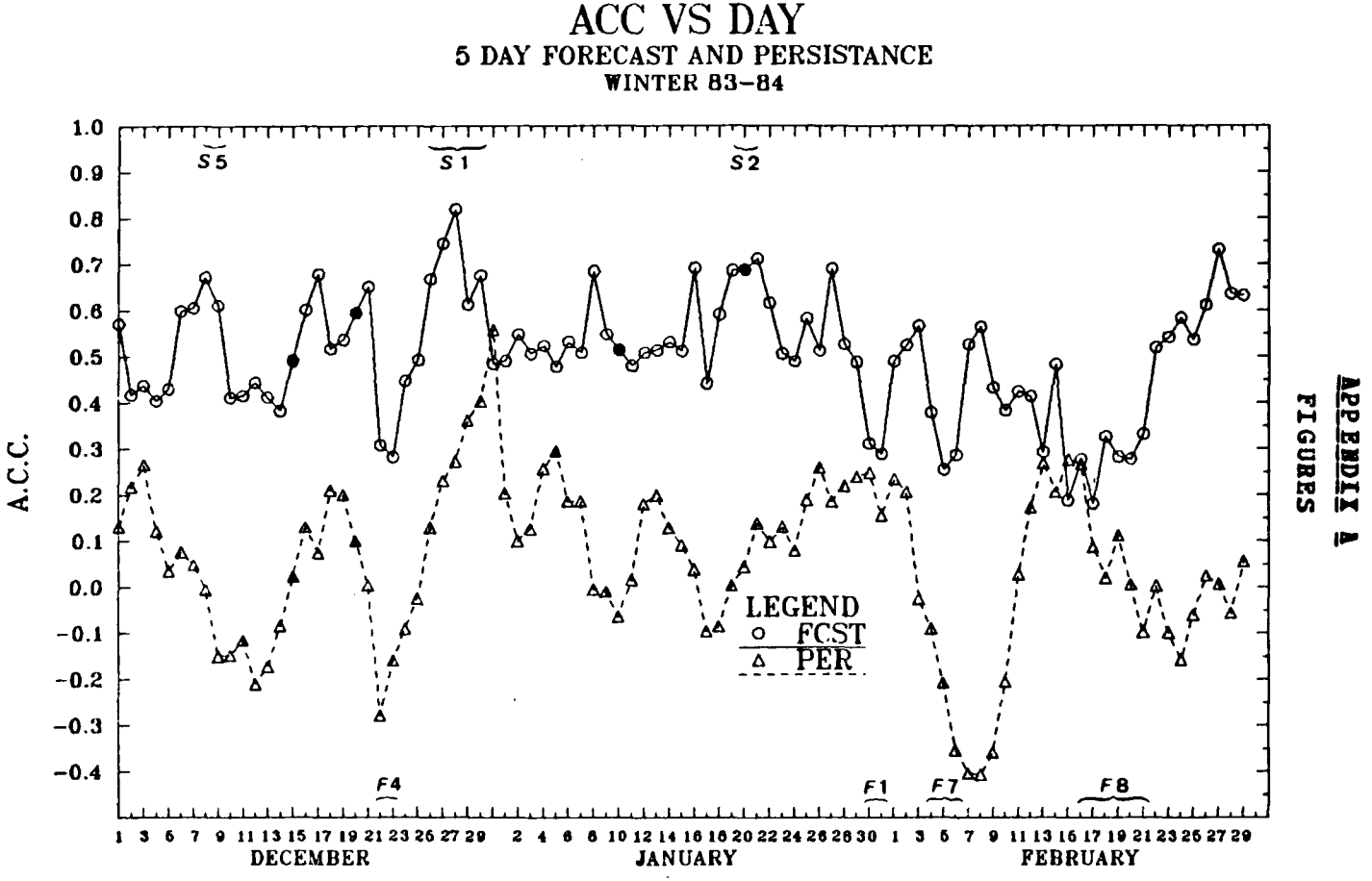

Fig. A.1 Winter 83-84 time series of five-day forecast ACC score plotted on forecast generation day. Shaded points are interpolated data.

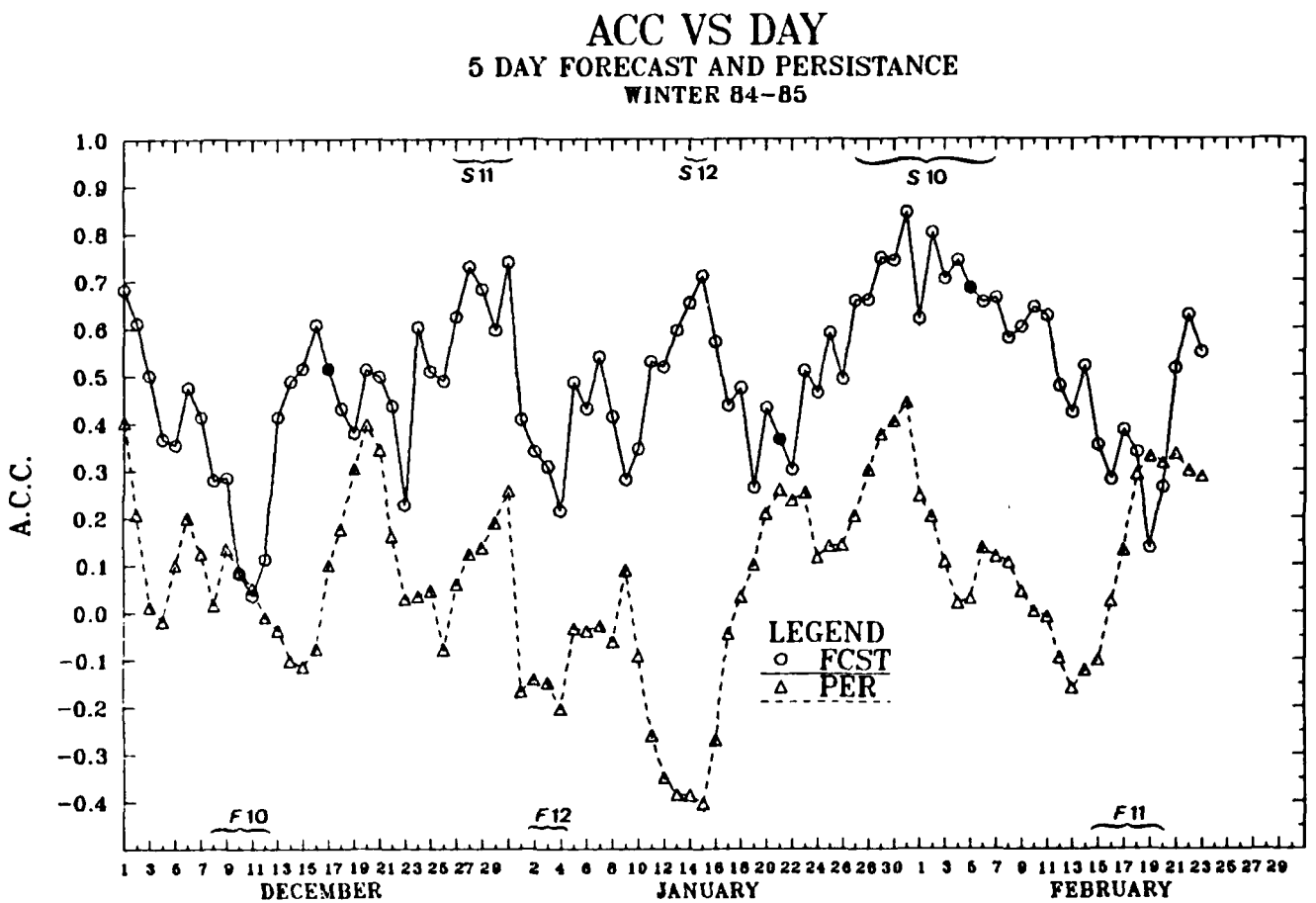

Fig. A.2 Winter 84-85 time series of five-day forecast ACC score plotted on forecast generation day. Shaded points are interpolated data.

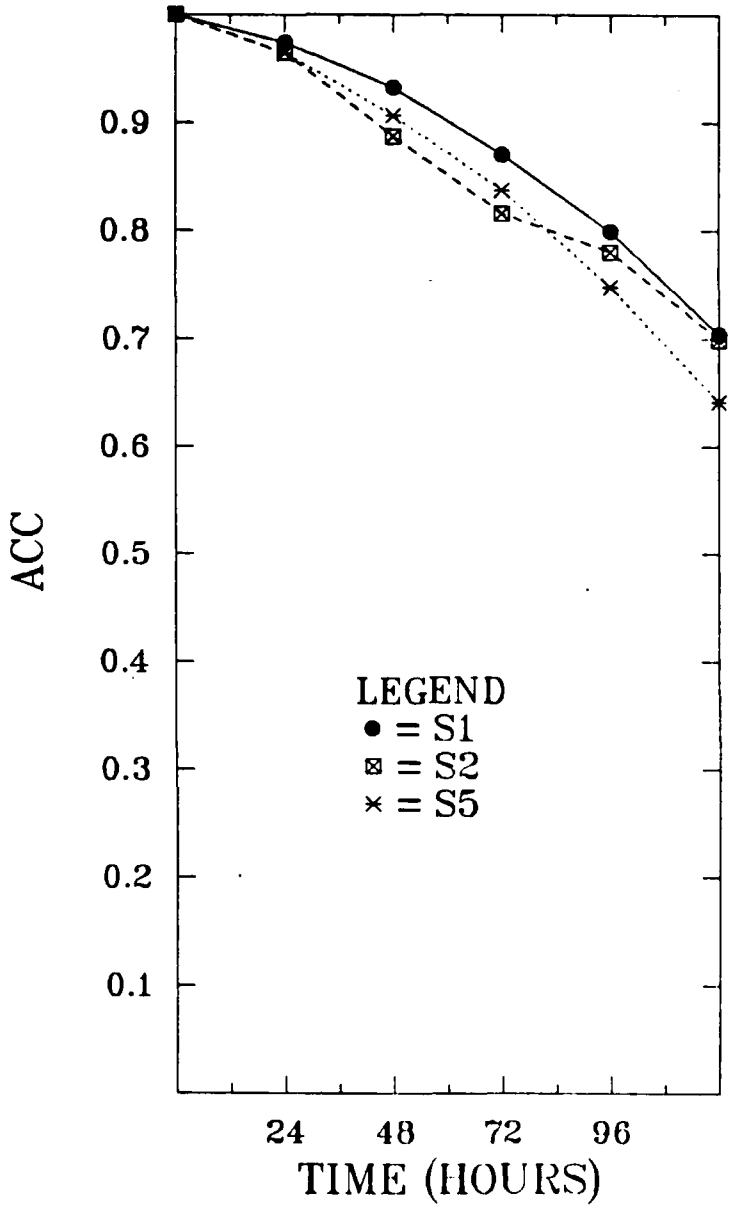

Fig. A.3 ACC versus forecast day for winter 1983-84 STARH periods. Each ACC value plotted represents an average value for the period.

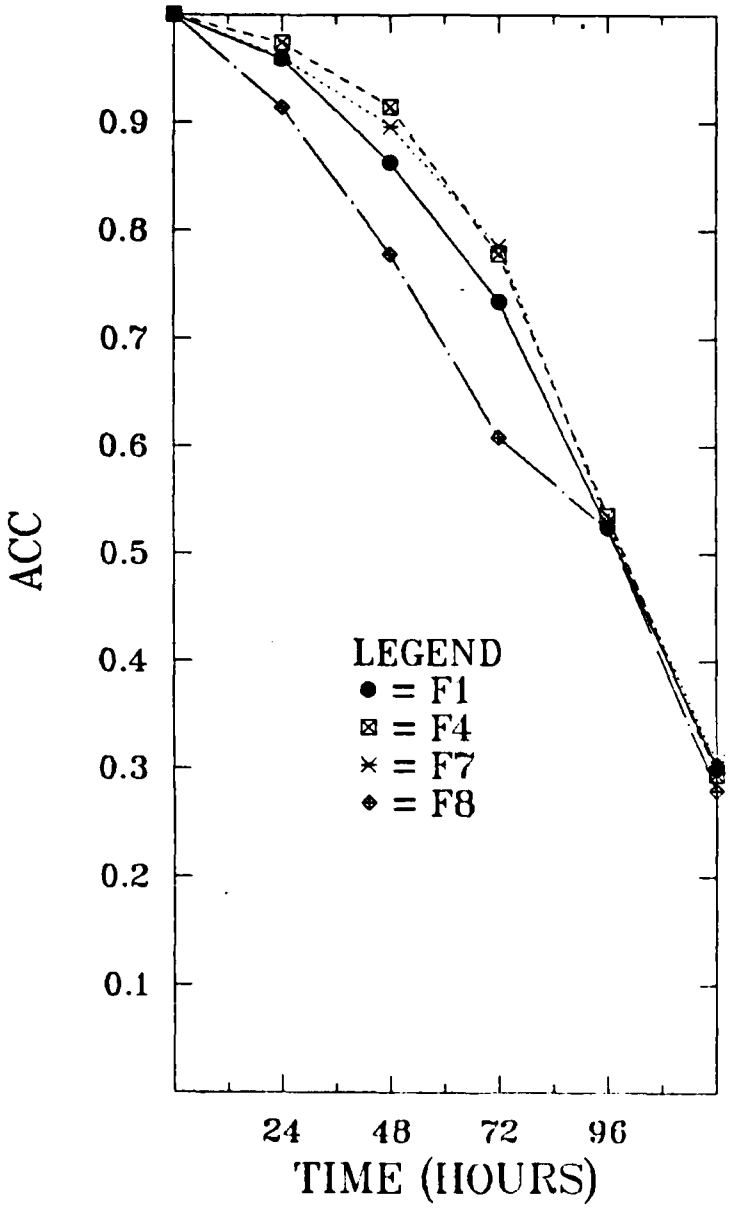

Fig. A.4 ACC versus forecast day for winter 1983-84 FLOP periods. Each ACC value plotted represents an average value for the period.

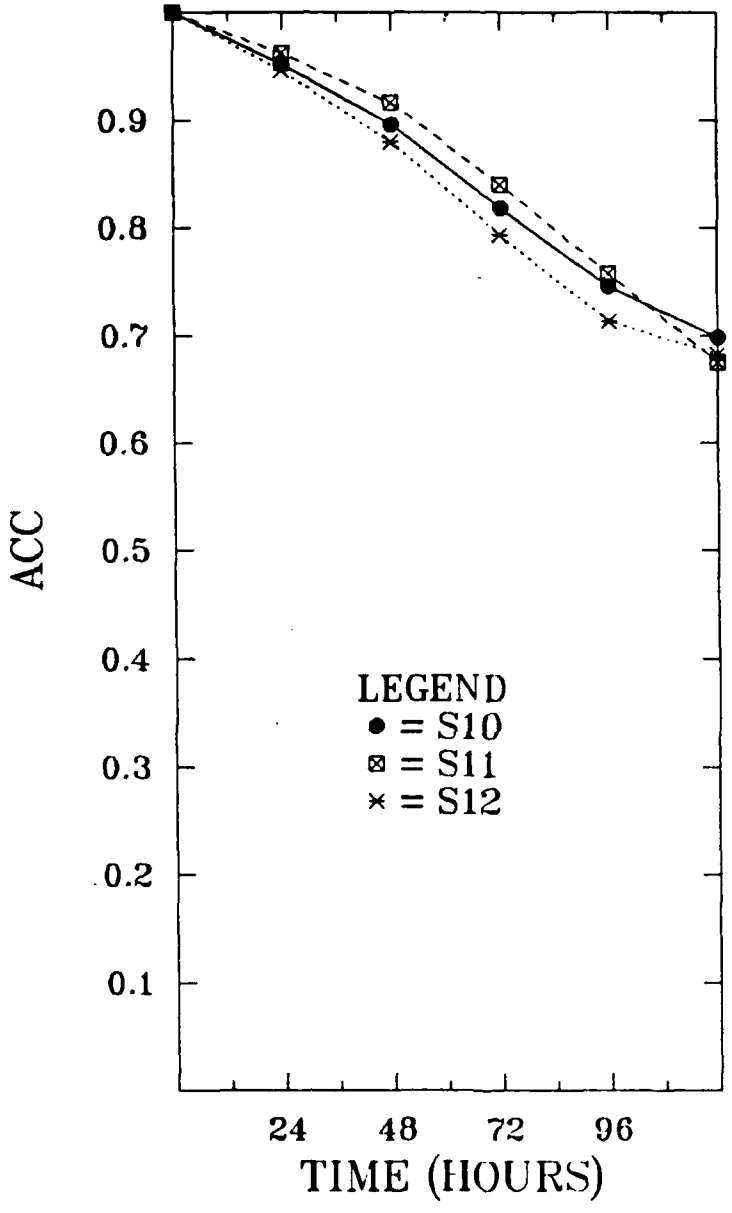

Fig. A.5 ACC versus forecast day for winter 1984-85 STARH periods. Each ACC value plotted represents an average value for the period.

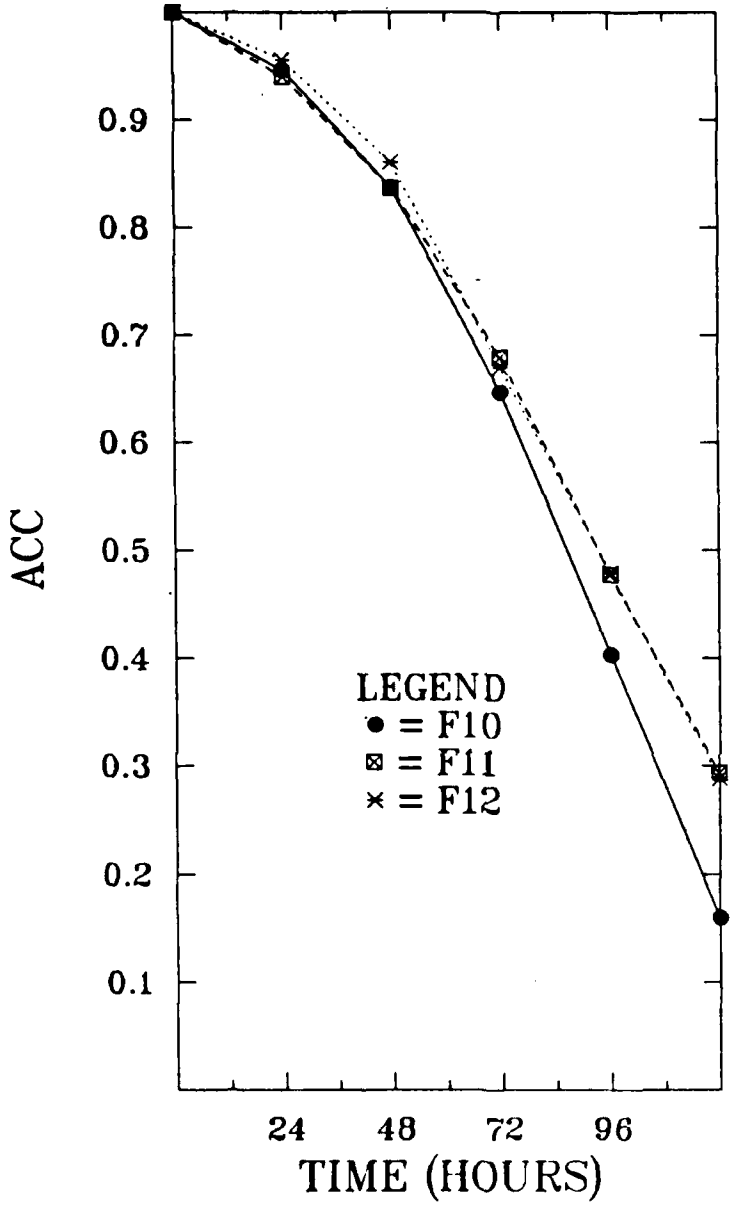

Fig. A.6 ACC versus forecast day for winter 1984-85 FLOP periods. Each ACC value plotted represents an average value for the period.

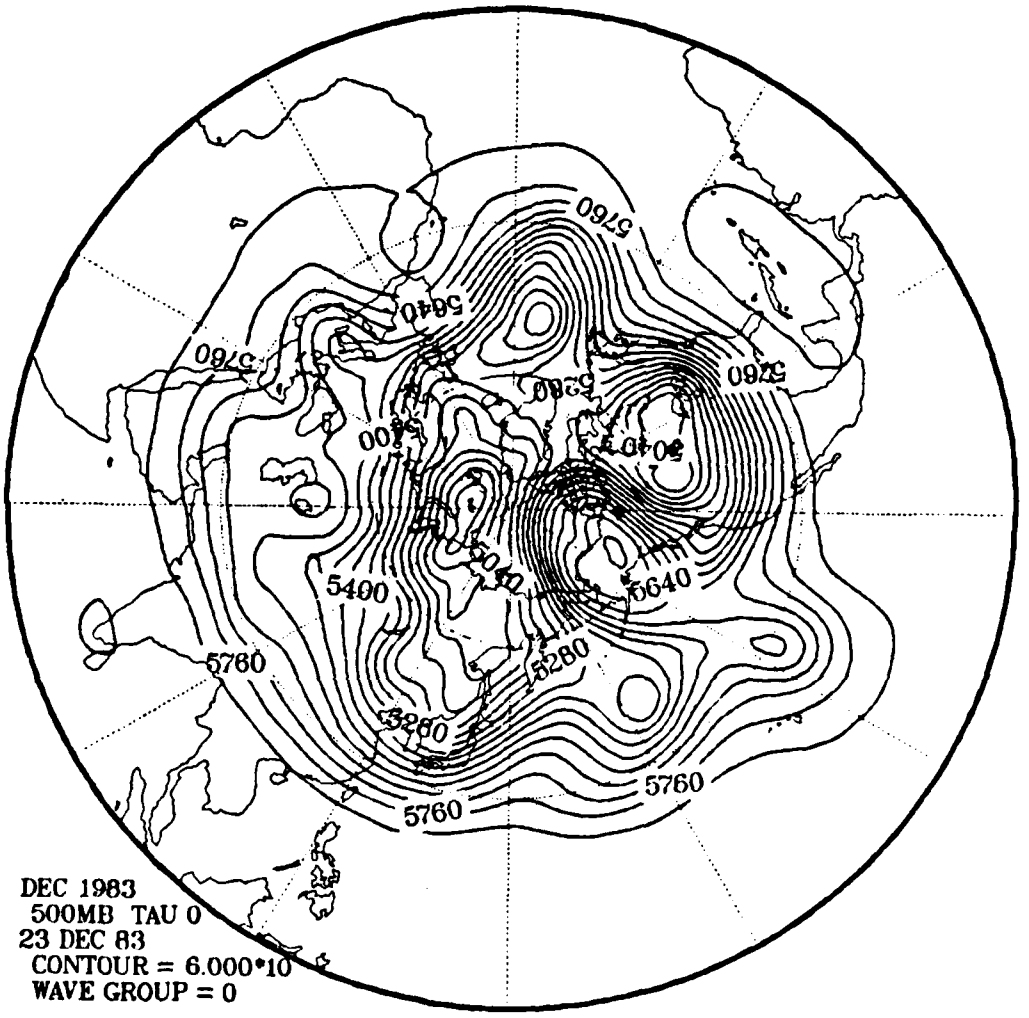

Fig. A.7 23 December 1983 500 mb height analysis, Northern Hemisphere Polar Stereographic projection.

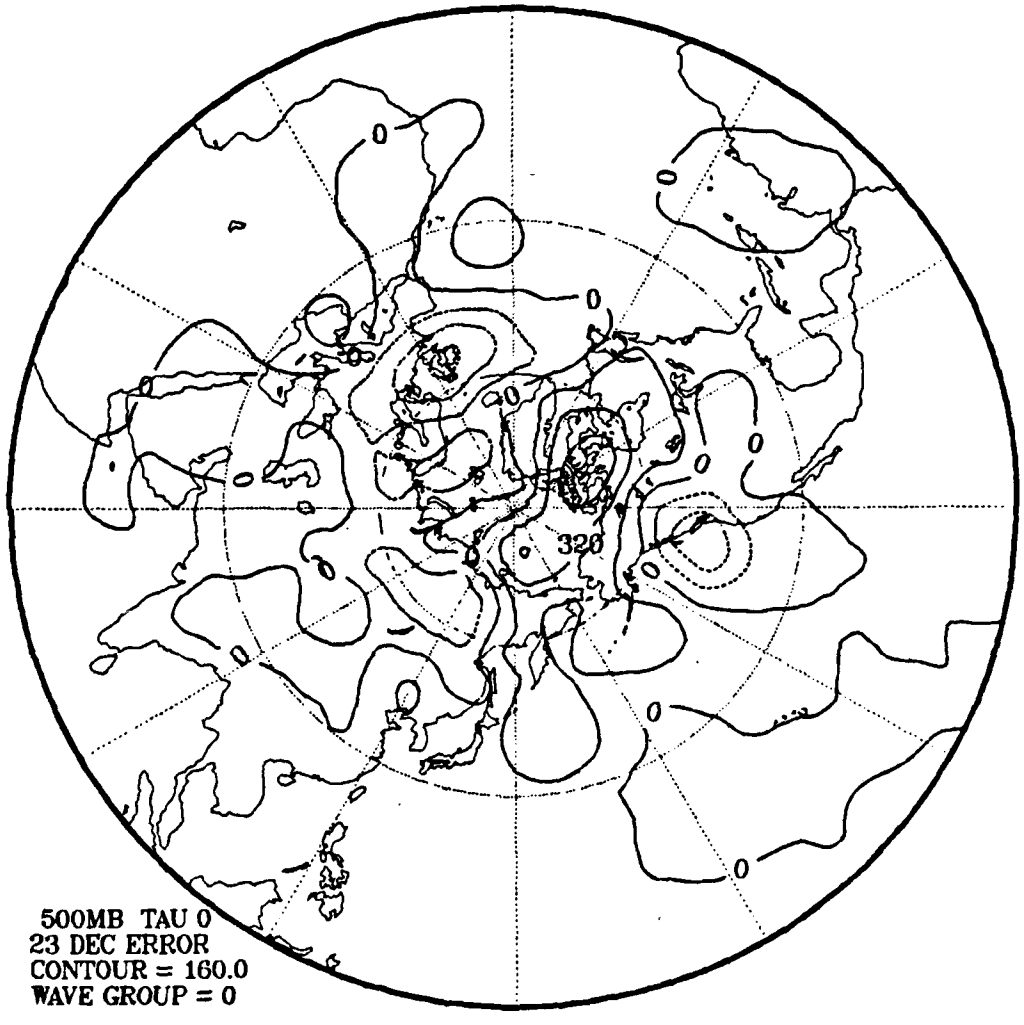

Fig. A.8 Error patterns for 23 December 1983 500 mb five-day forecast field minus 28 December 1983 500 mb analysis field.

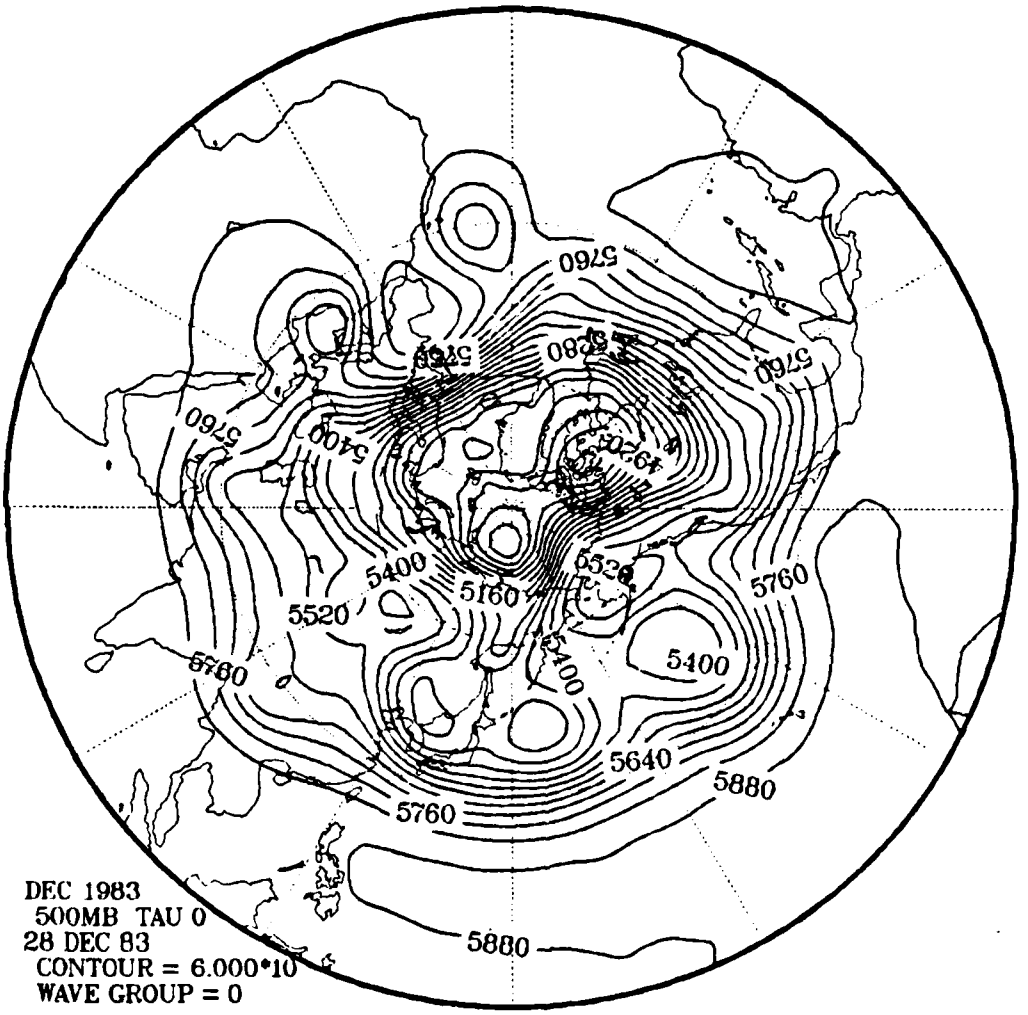

Fig. A.9 28 December 1983 500 mb height analysis, Northern Hemisphere Polar Stereographic projection.

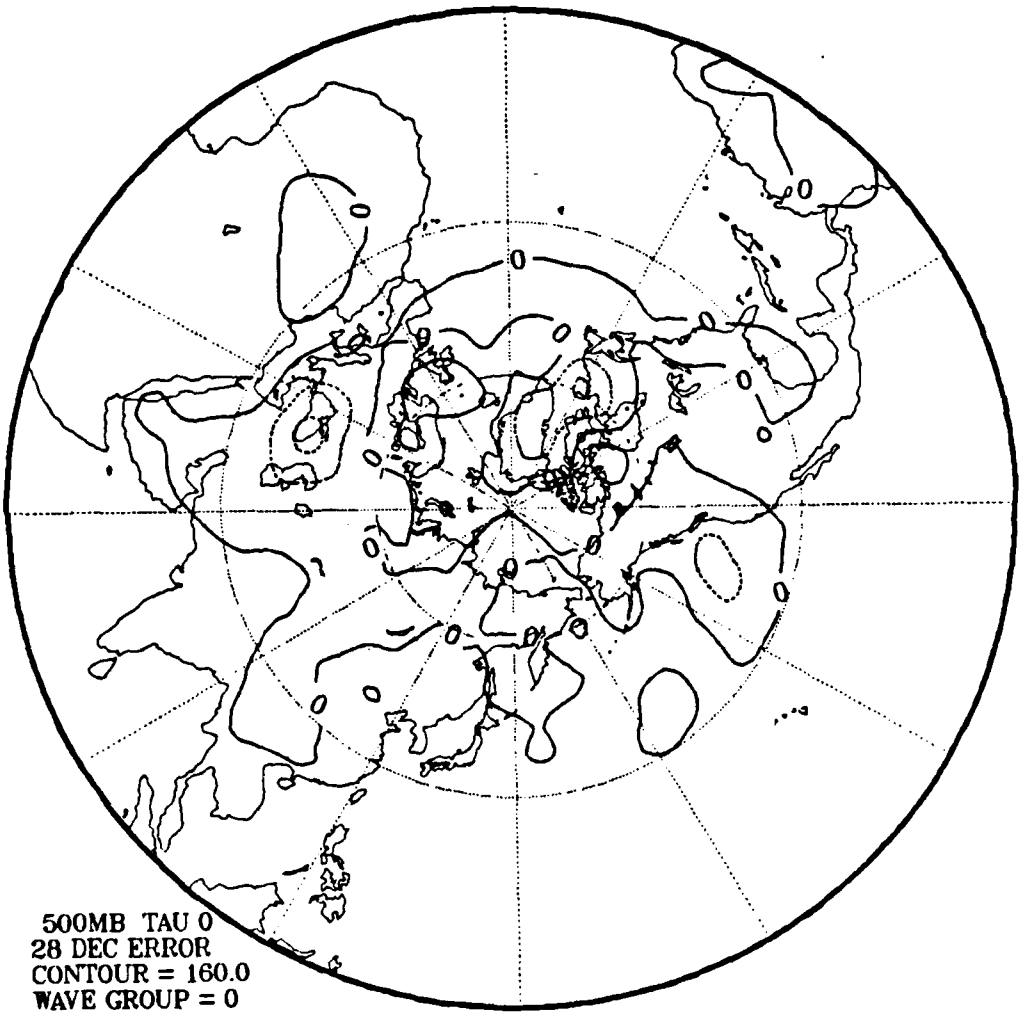

Fig. A.10 Error patterns for 28 December 1983 500 mb five-day forecast field minus 02 January 1984 500 mb analysis field.

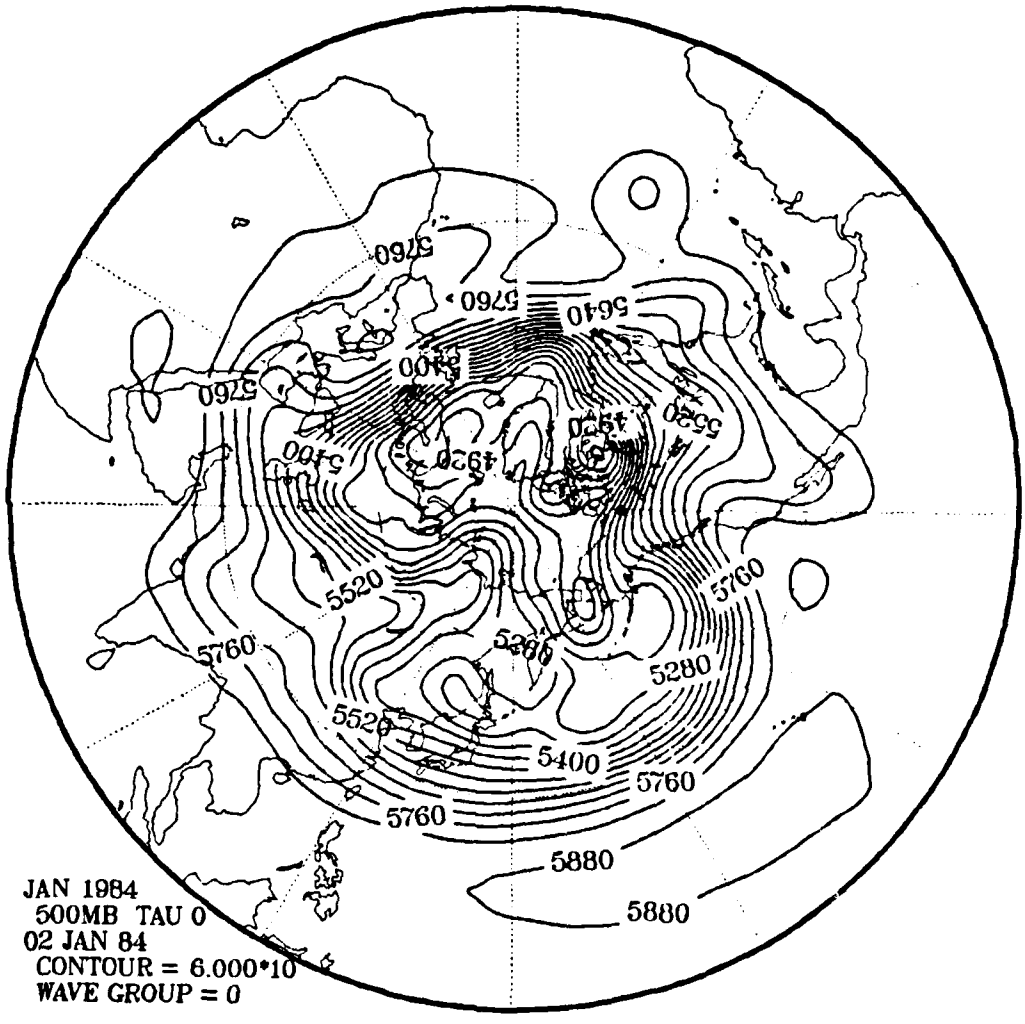

Fig. A.11 02 January 1984 500 mb height analysis, Northern Hemisphere Polar Stereographic projection.

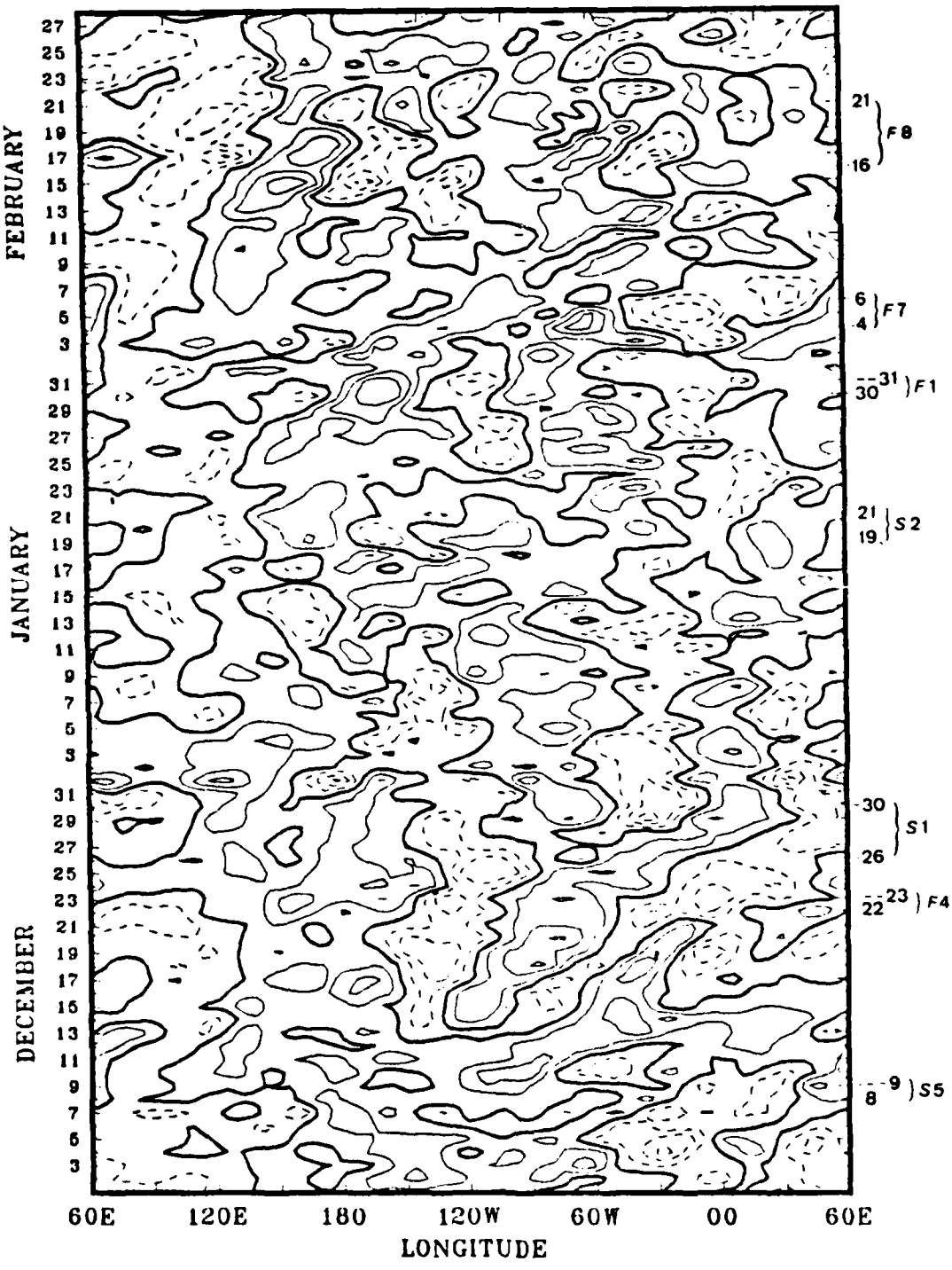

Fig. A.12 Winter 1983-84 day-five error patterns (average five-day forecast 500 mb heights minus average verifying day an heights).

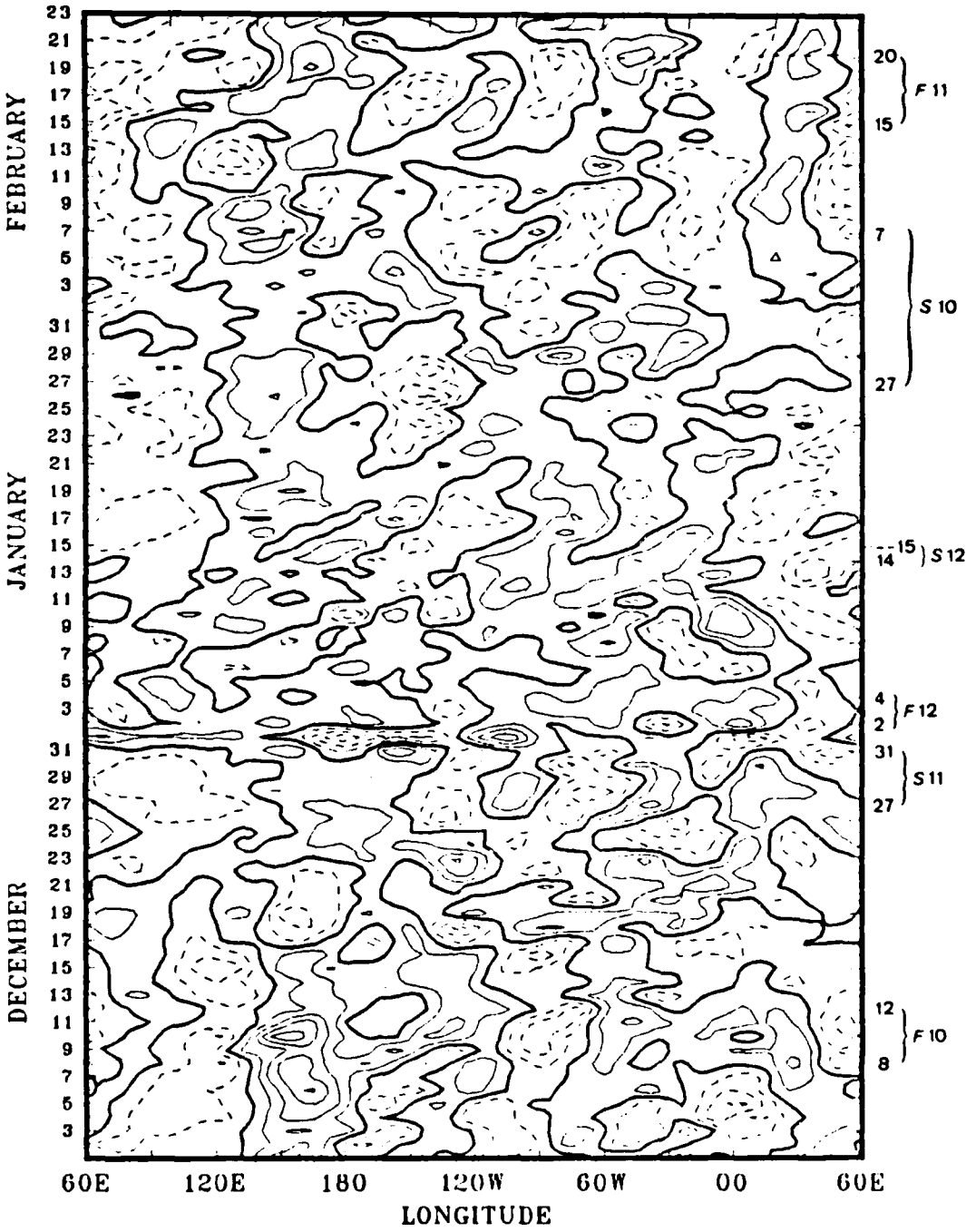

Fig. A.13 Winter 1984-85 day-five error patterns (average five-day forecast 500 mb heights minus average verifying day an heights).

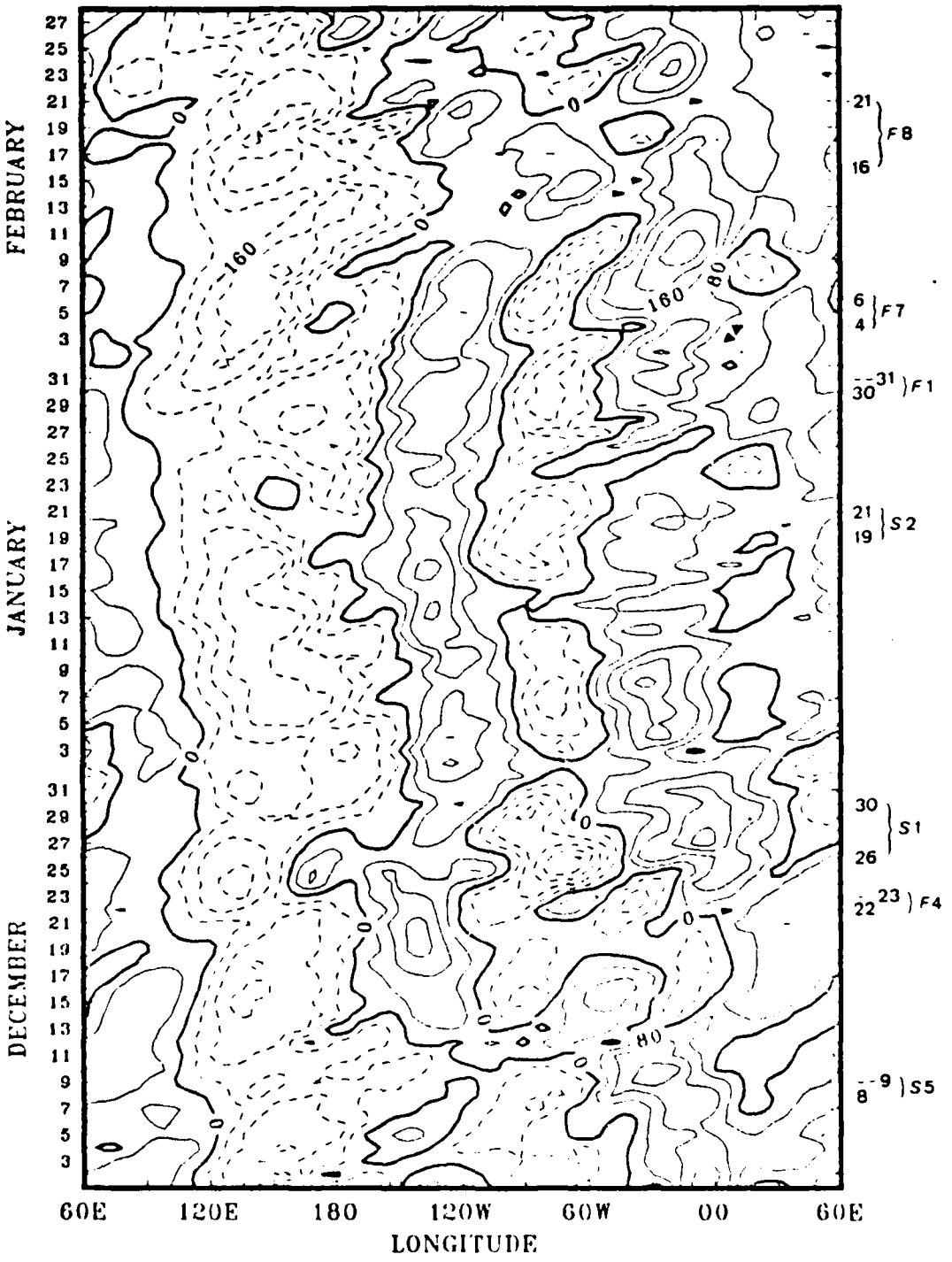

Fig. A.14 Winter 1983-84 average daily 500 mb analysis heights averaged over latitude band 30 to 60 degrees north.

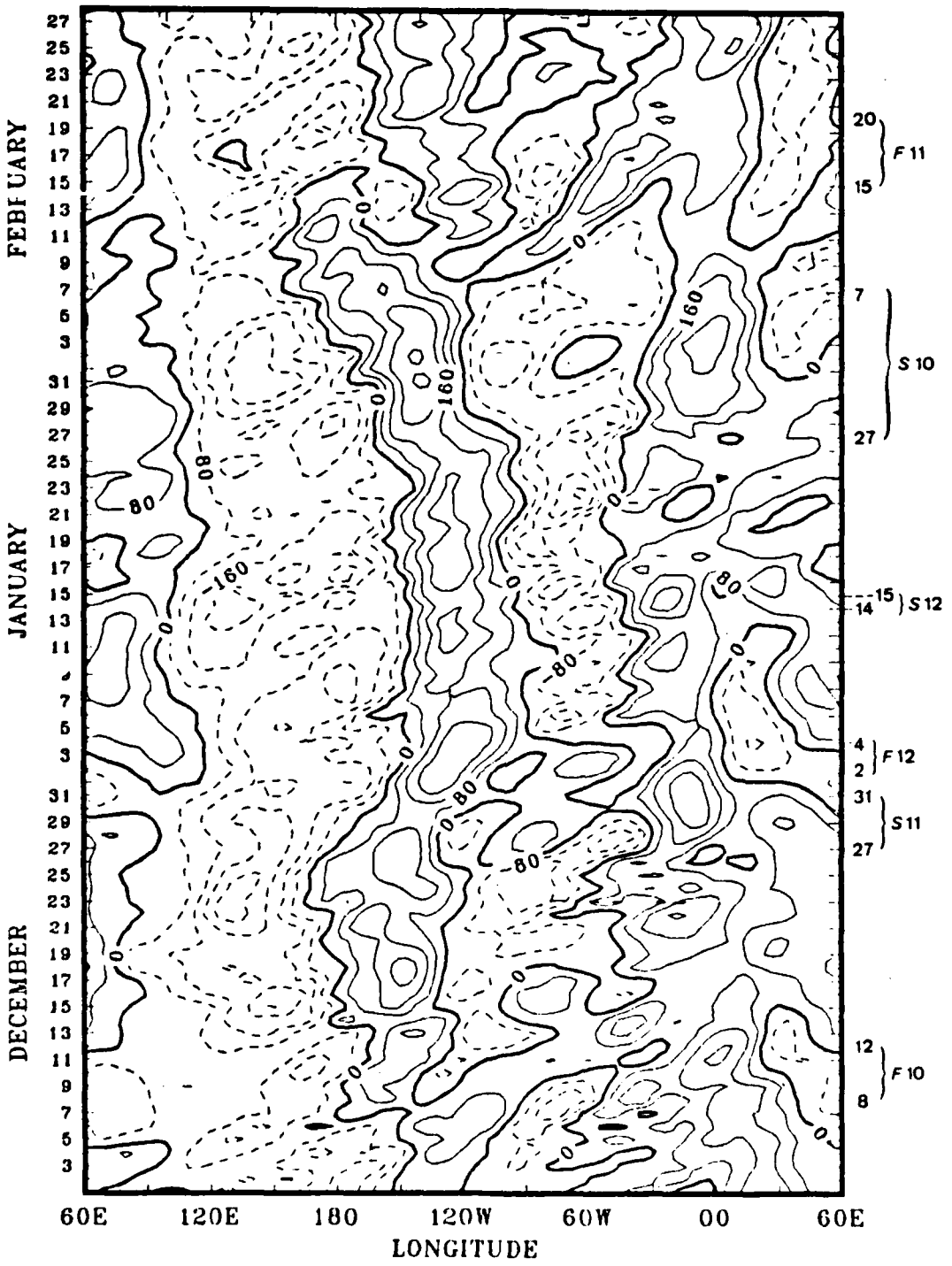

Fig. A.15 Winter 1984-85 average daily 500 mb analysis heights averaged over latitude band 30 to 60 degrees north.

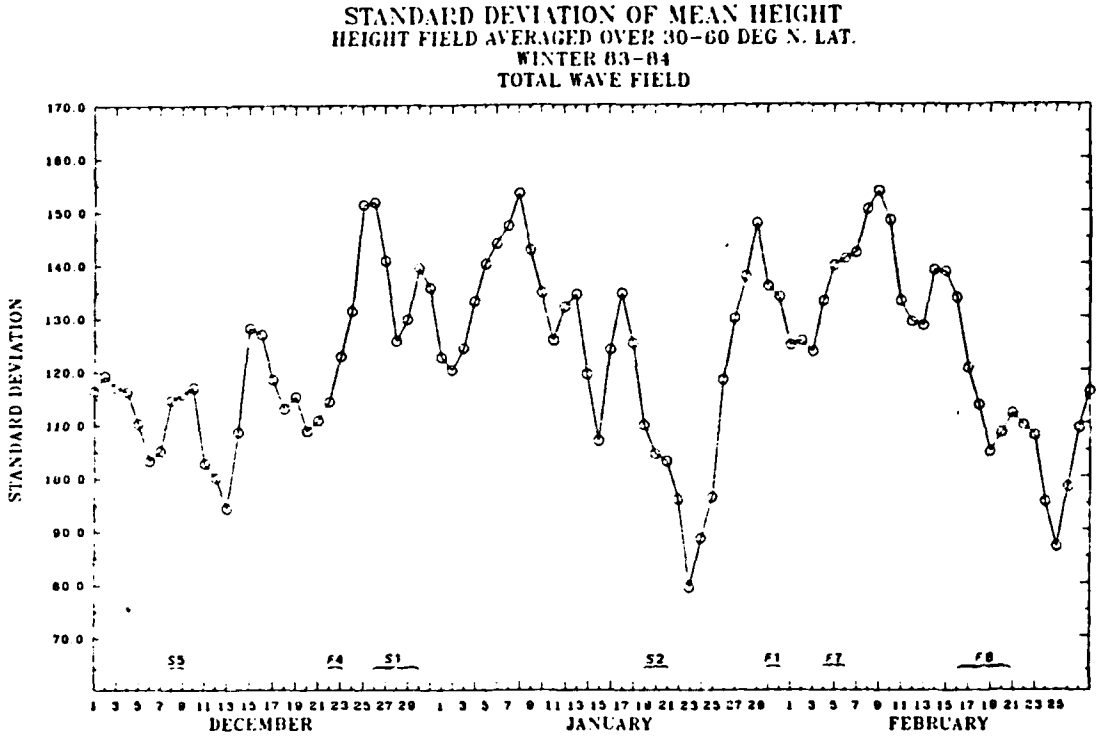

Fig. A.16 Winter 1983-84 Standard deviation of average daily 500 mb analysis heights of Figure A.14.

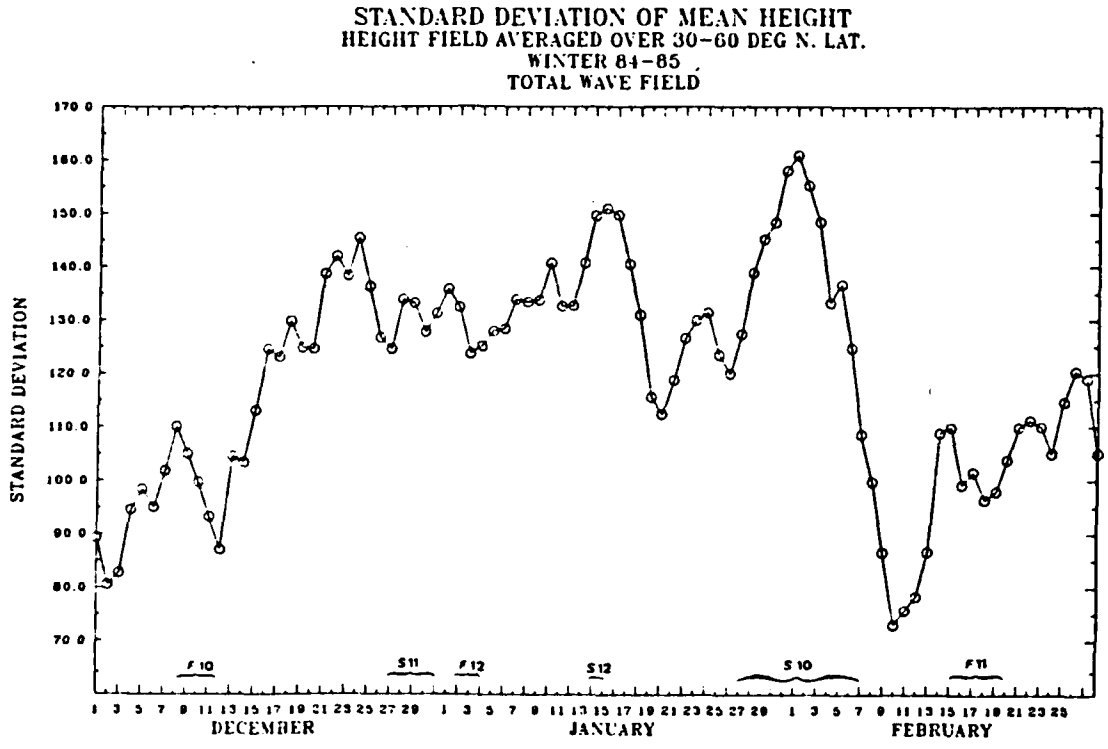

Fig. A.17 Winter 1984-85 Standard deviation of average daily 500 mb analysis heights of Figure A.15.

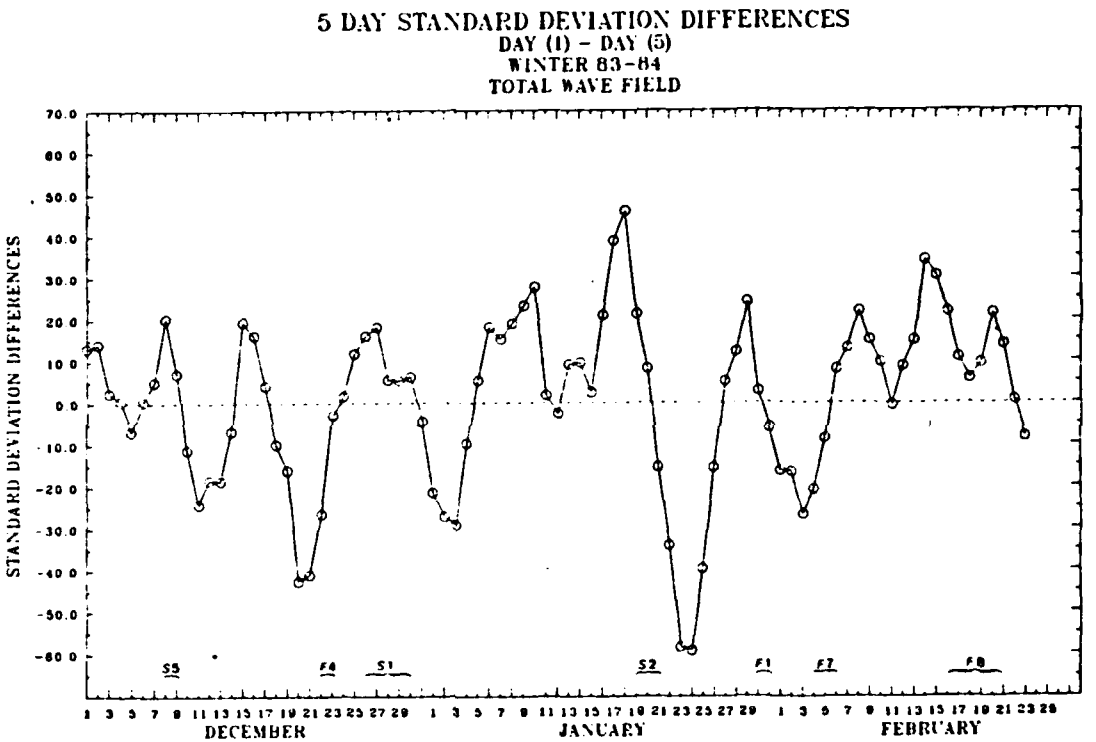

Fig. A.18 Winter 1983-84 five day standard deviation tendencies. Day-1 minus day-5 difference value plotted as a function of day one.

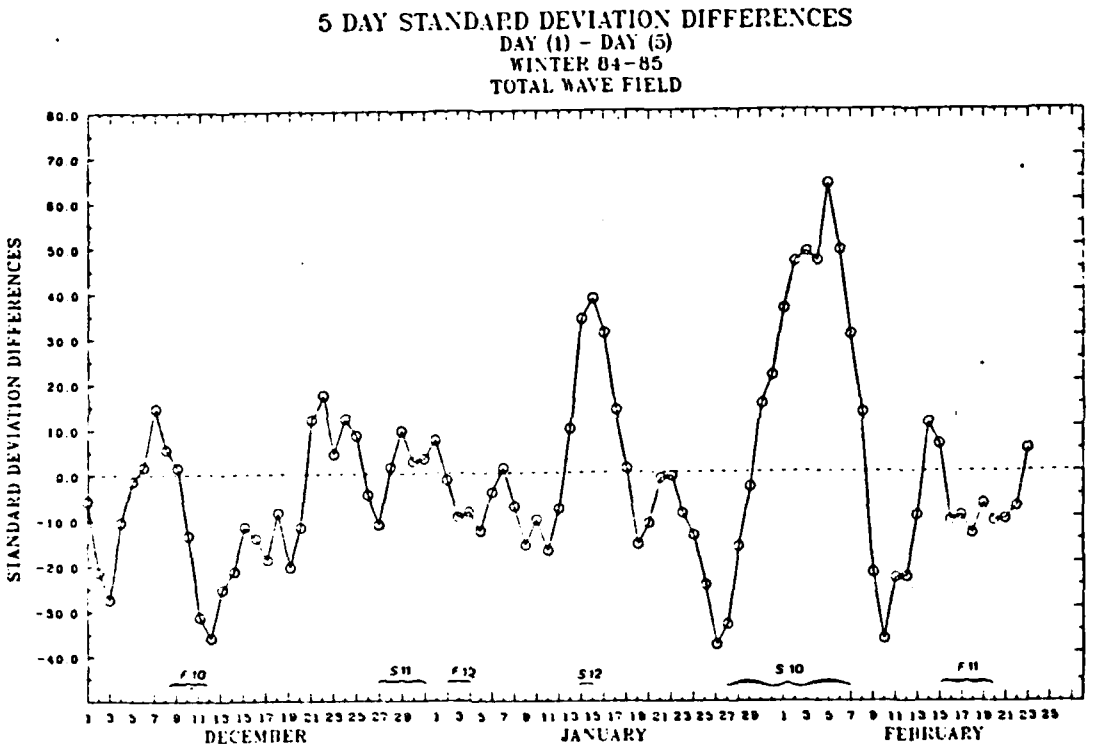

Fig. A.19 Winter 1984-85 five day standard deviation tendencies. Day-1 minus day-5 difference value plotted as a function of day one.

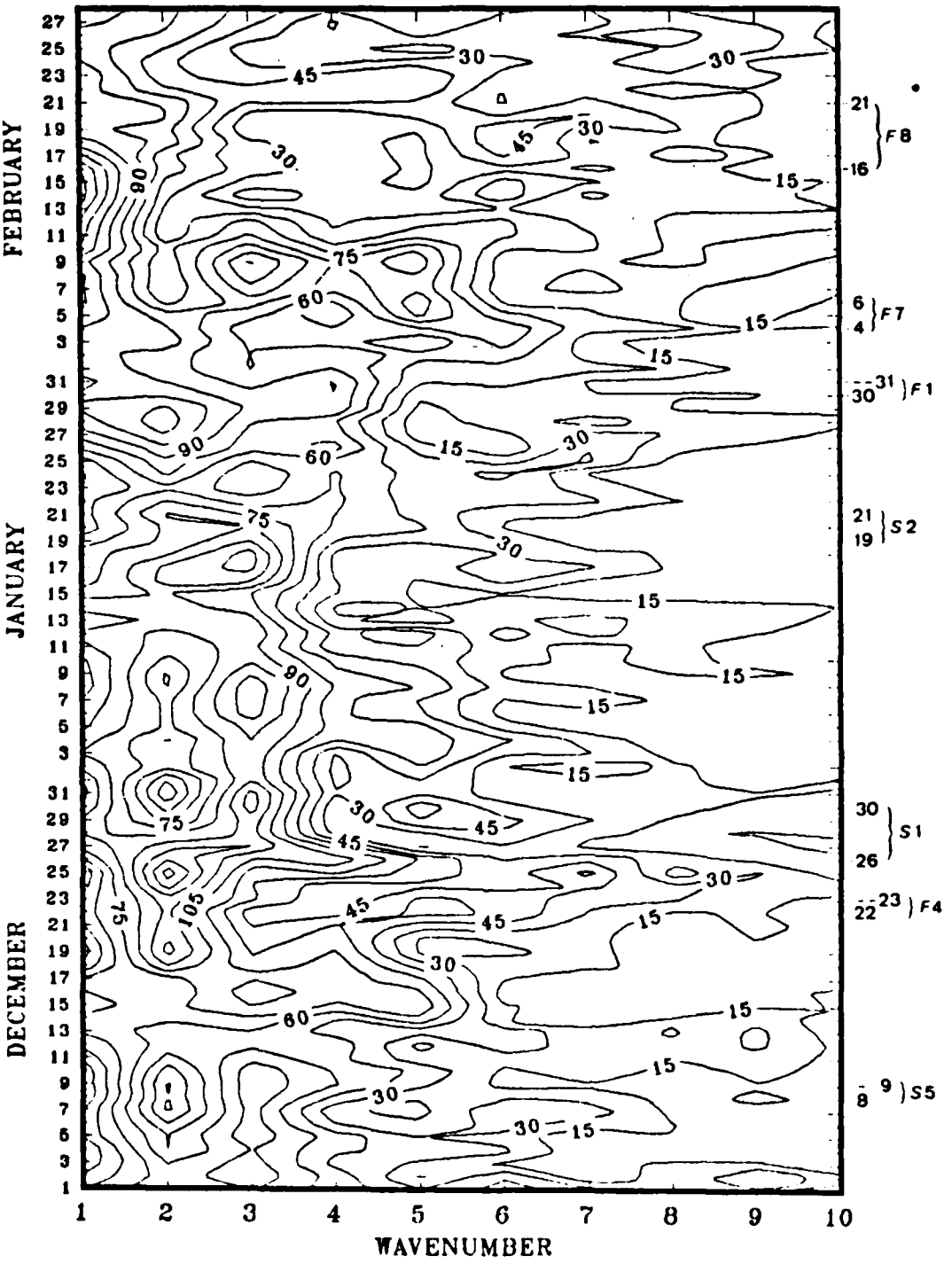

Fig. A.20 Winter 1983-84. Amplitude of zonal wavenumbers of average daily 500 mb height fields from Figure A.14.

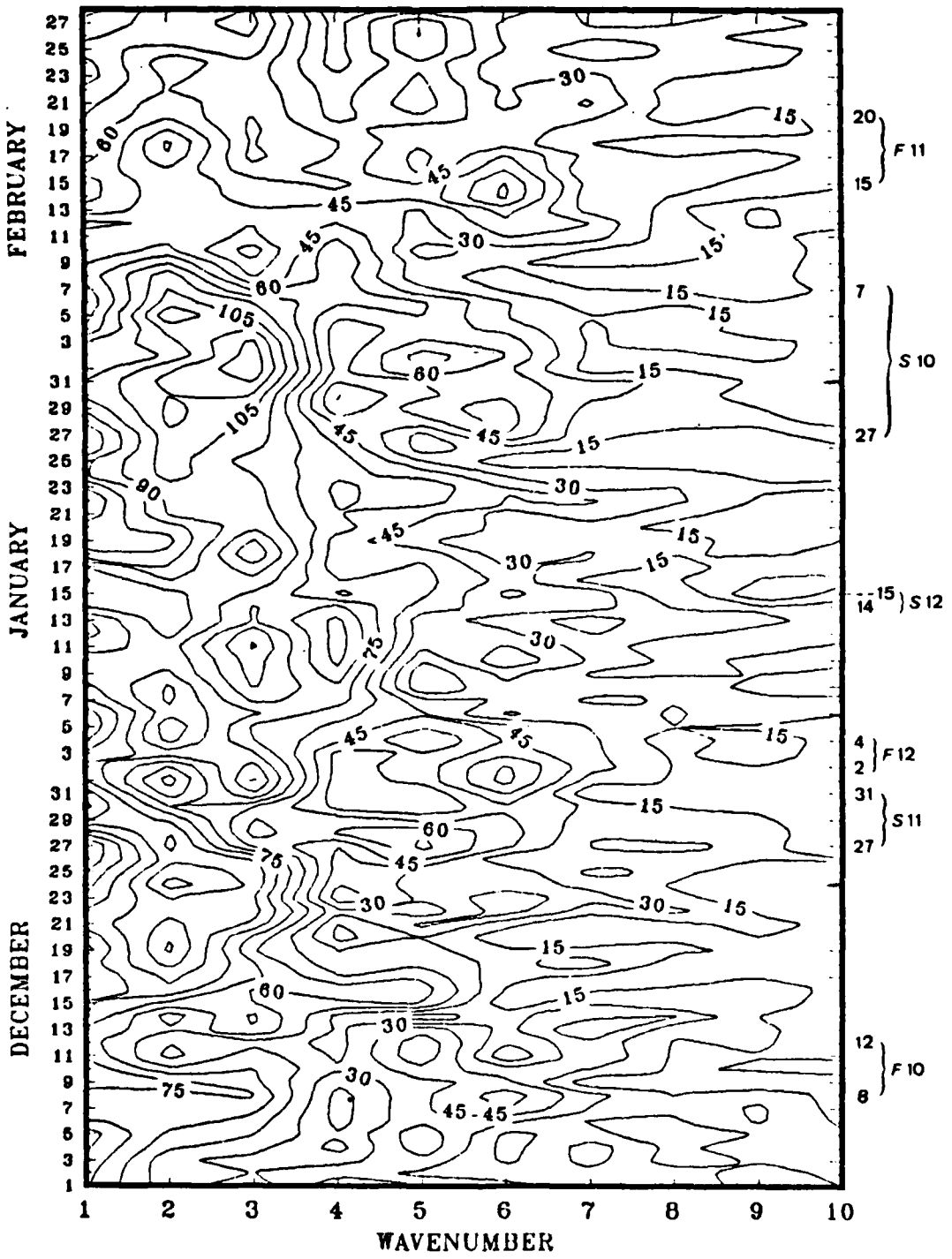

Fig. A.21 Winter 1984-85. Amplitude of zonal wavenumbers of average daily 500 mb height fields from Figure A.15.

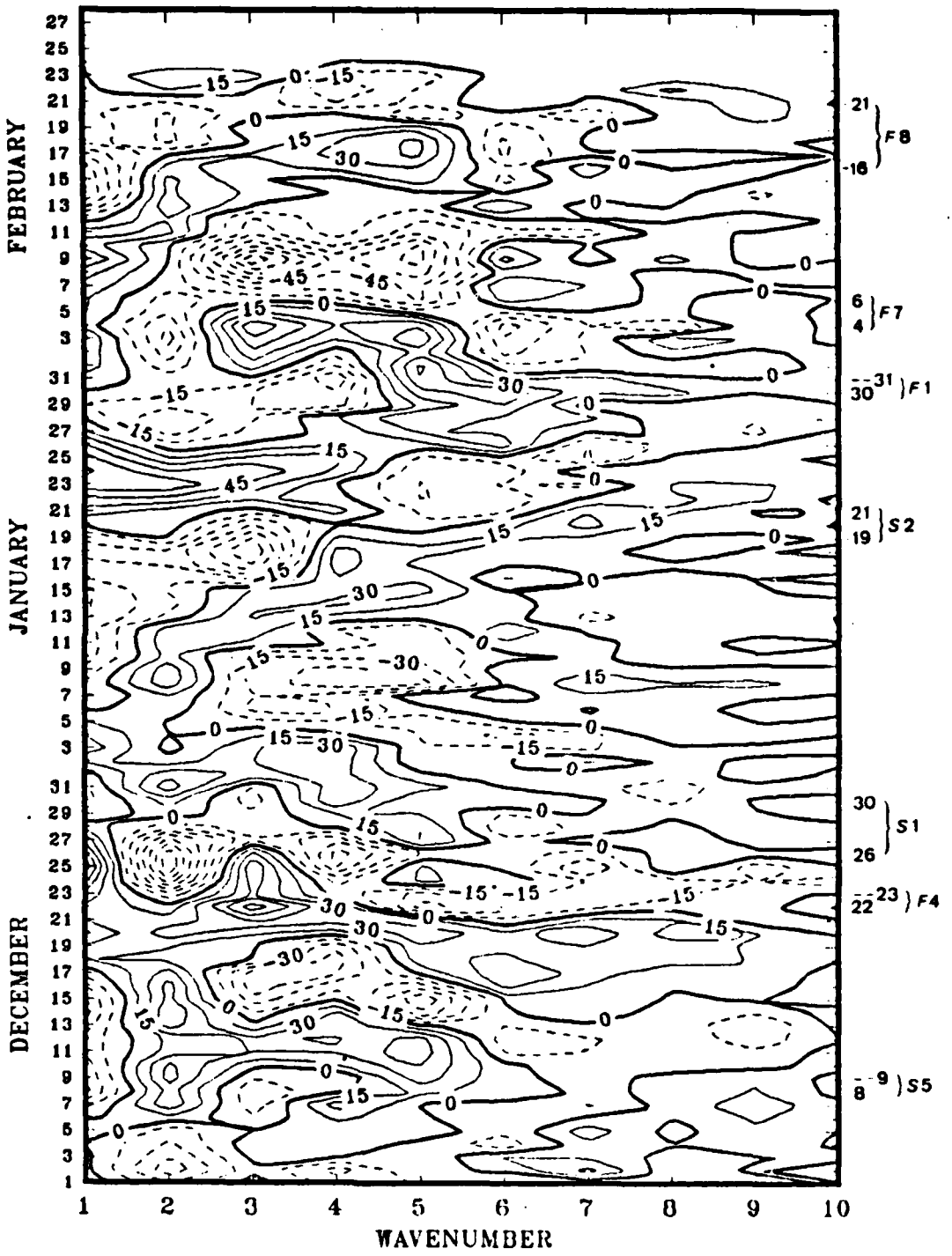

Fig. A.22 Winter 1983-84. Five-day amplitude tendencies of zonal wavenumbers. Day-5 minus day-1 differences plotted as a function of day one.

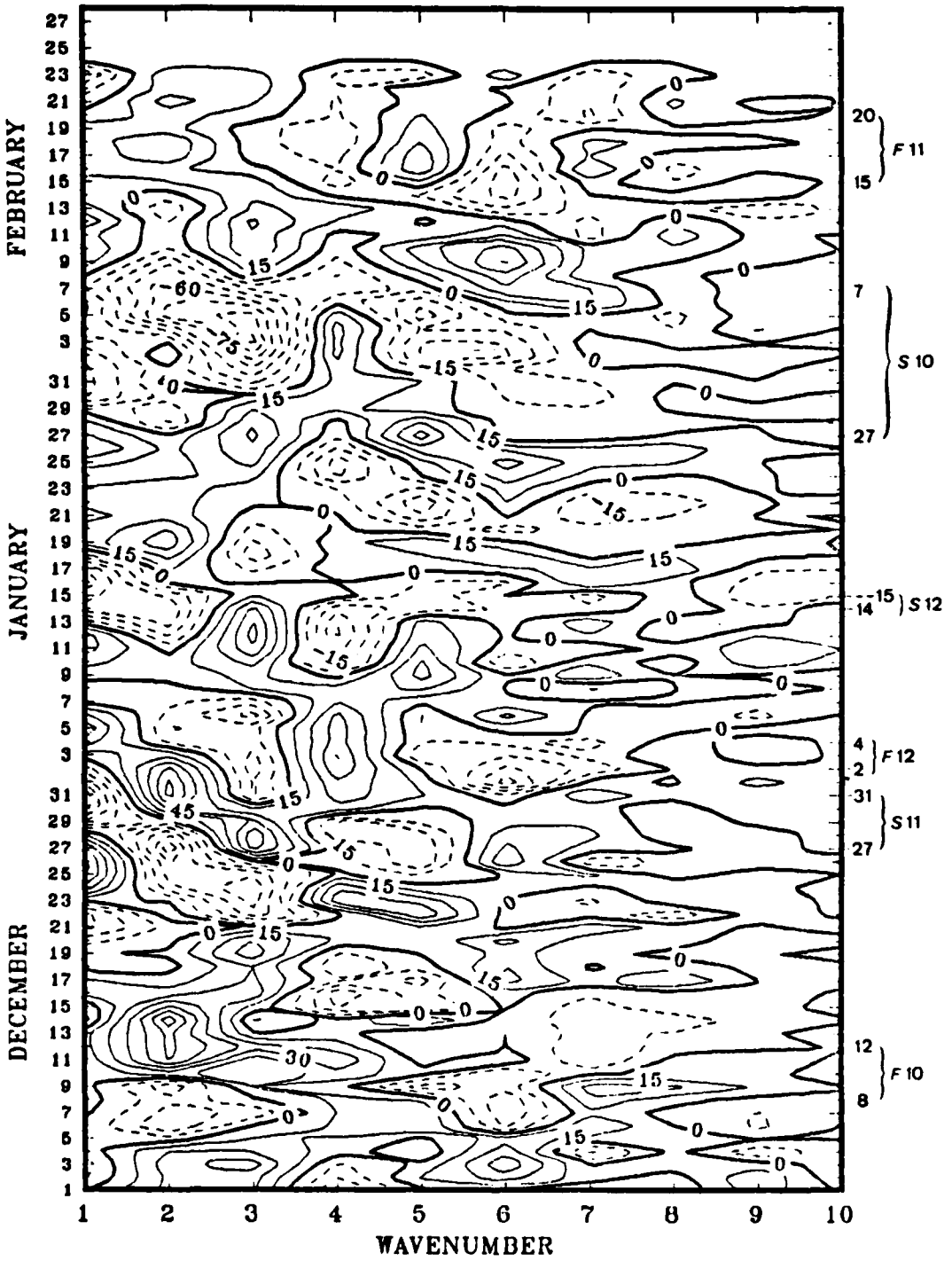

Fig. A.23 Winter 1984-85. Five-day amplitude tendencies of zonal wavenumbers. Day-5 minus day-1 differences plotted as a function of day one.

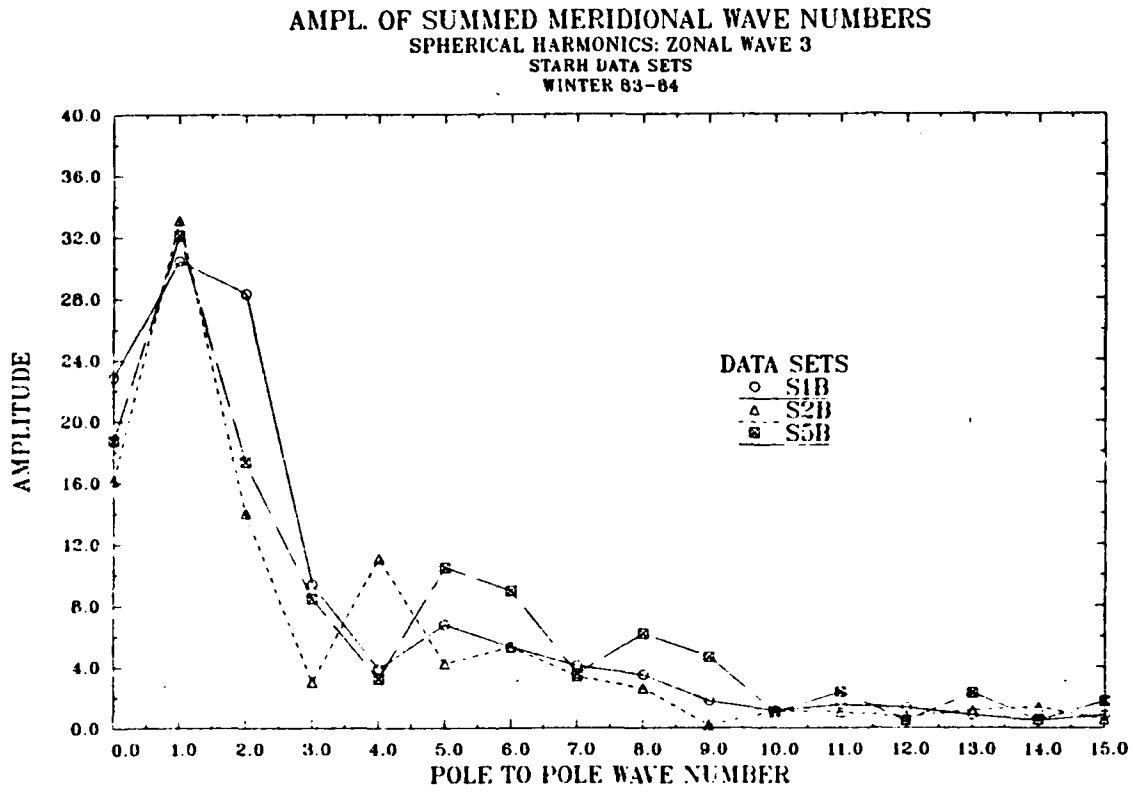

Fig. A.24 Winter 1983-84. Pole to pole wavenumber amplitude of zonal wave 3 for STARH periods.

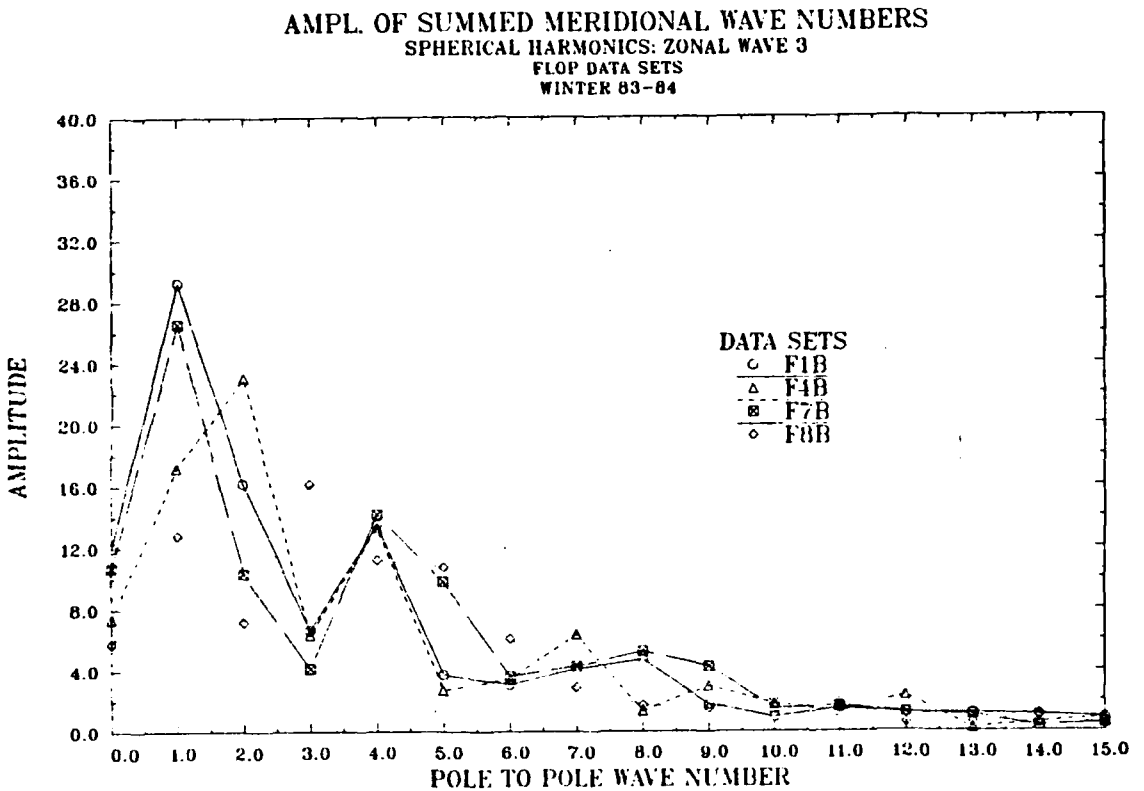

Fig. A.25 Winter 1983-84. Pole to pole wavenumber amplitude of zonal wave 3 for FLOP periods.

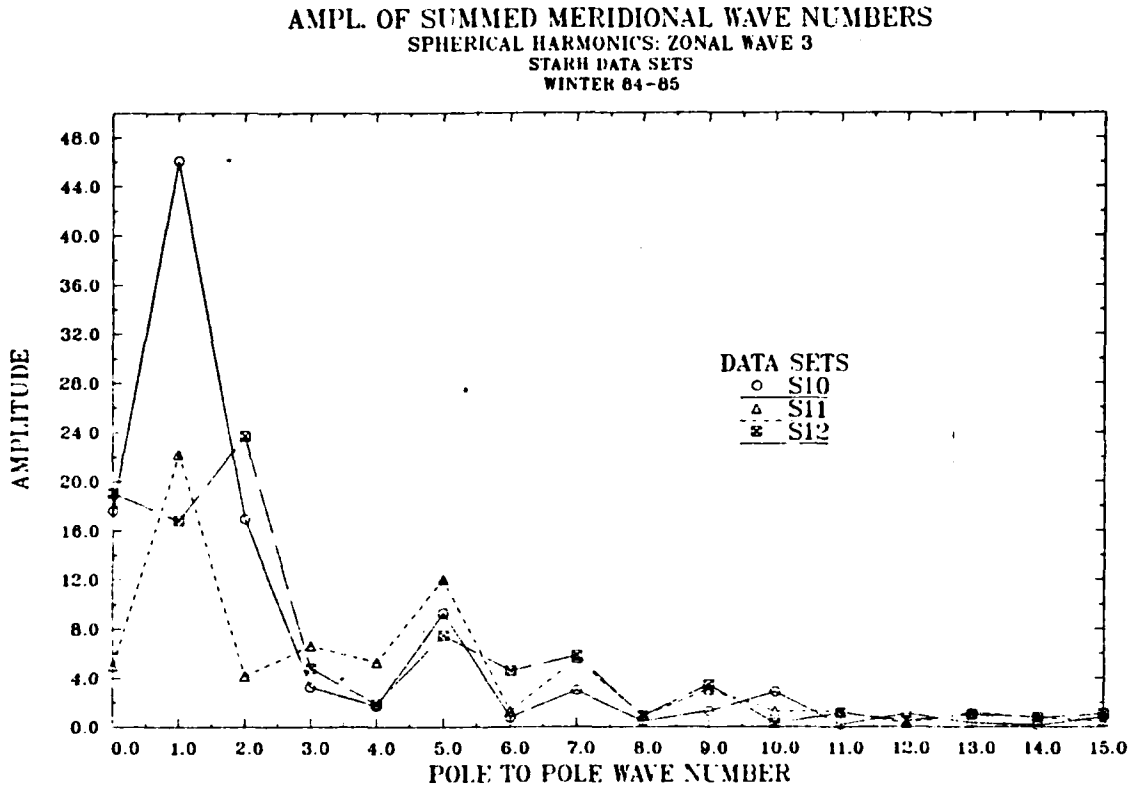

Fig. A.26 Winter 1984-85. Pole to pole wavenumber amplitude of zonal wave 3 for STARH periods.

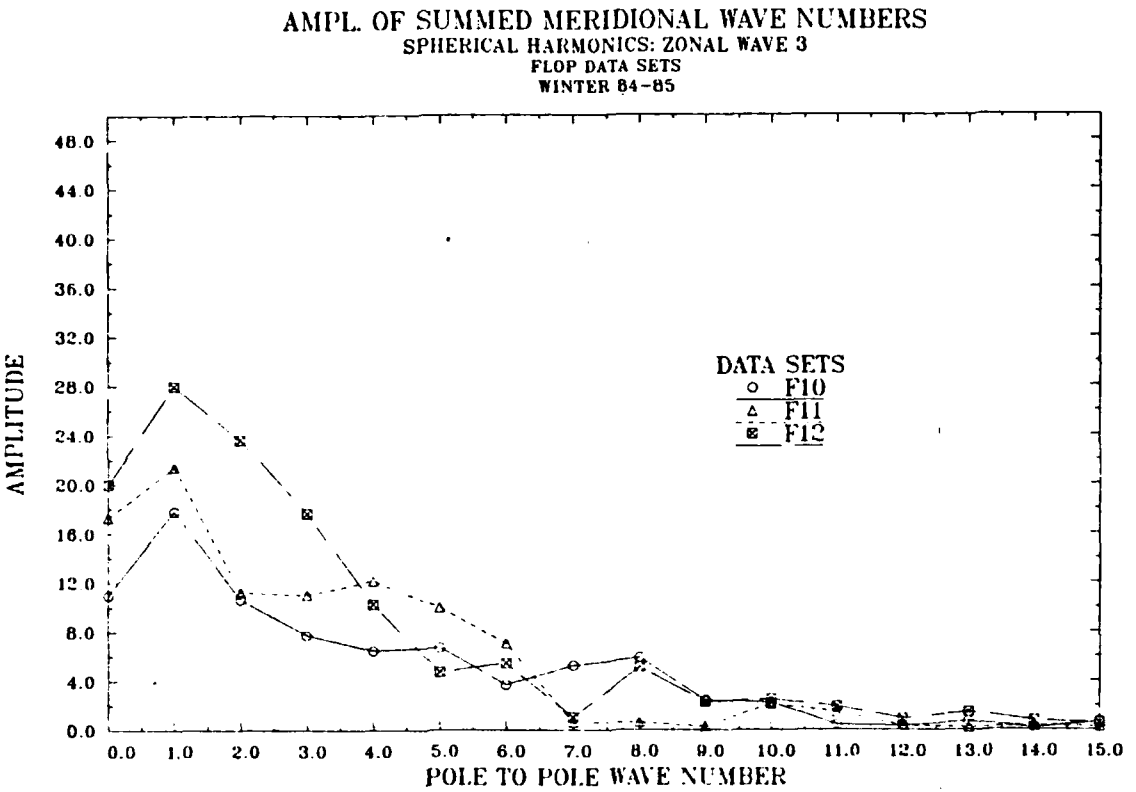

Fig. A.27 Winter 1984-85. Pole to pole wavenumber amplitude of zonal wave 3 for FLOP periods.

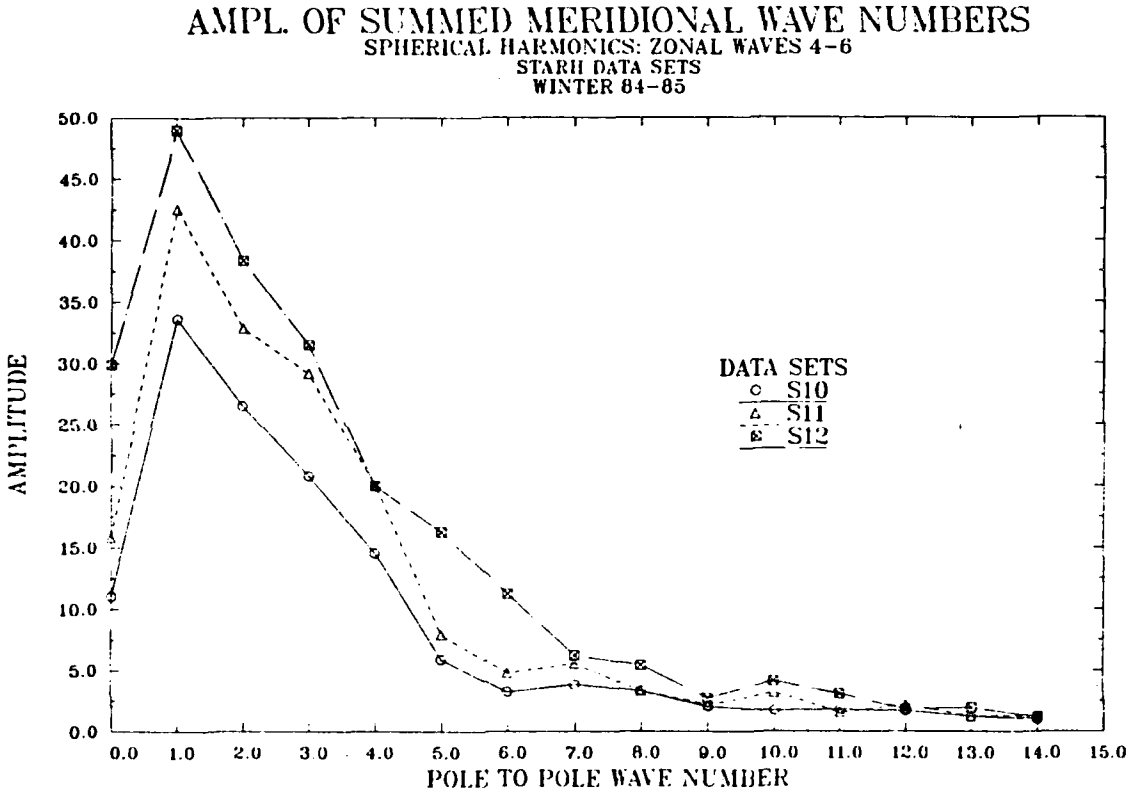

Fig. A.28 Winter 1984-85. Pole to pole wavenumber amplitude of summed zonal waves 4, 5 and 6 for STARH periods.

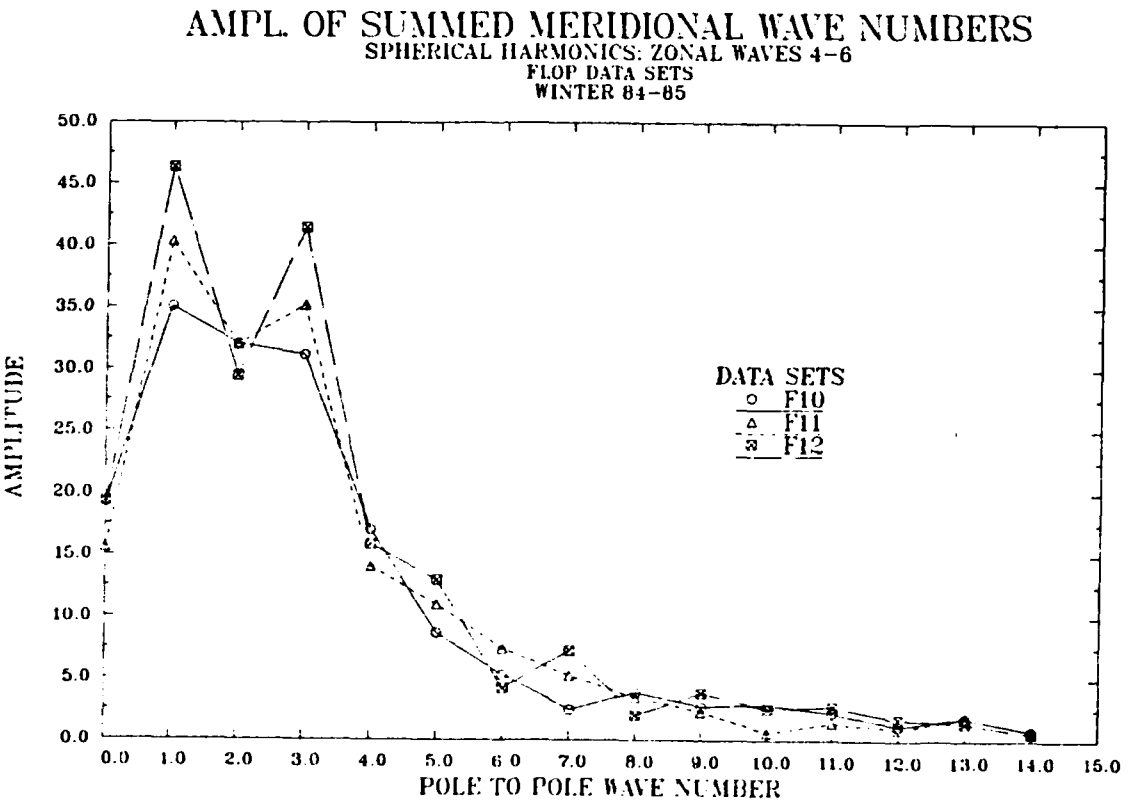

Fig. A.29 Winter 1984-85. Pole to pole wavenumber amplitude of summed zonal waves 4, 5 and 6 for FLOP periods.

APPENDIX B

TABLES

TABLE 1

SUMMARY OF SELECTED PERIODS

Winter	Period	Days when 5 day forecasts were generated	Average ACC of period
83-84	S1	26-30 Dec 83	0.705
	S2	19-21 Jan 84	0.699
	S5	08-09 Dec 83	0.642
Avg.= 0.500 S.D.= 0.134	F1	30-31 Jan 84	0.301
	F4	22-23 Dec 83	0.295
	F7	04-06 Feb 84	0.250
	F8	16-21 Feb 84	0.267
84-85	S10	27 Jan-07 Feb 1985	0.713
	S11	27-31 Dec 84	0.675
	S12	14-15 Jan 85	0.678
Avg.= 0.490 S.D.= 0.171	F10	08-12 Dec 84	0.160
	F11	15-20 Feb 85	0.281
	F12	02-04 Jan 85	0.288

TABLE 2

SUMMARY OF ANALYSIS RESULTS

WINTER	PERIOD	Persistence Errors	Early Standard Deviation Differences	Zonal Wavenumber Differences	SPHERICAL HARMONICS Zonal Wave 3	SPHERICAL HARMONICS Zonal Waves 4-6
83-84	S1	X	-	X	/	X	-
	S2	O	-	/	X	X	-
	S5	O	-	X	/	X	-
	F1	O	-	/	X	X	-
	F4	X	-	/	X	X	-
	F7	X	-	/	/	X	-
	F8	O	X	O	O	X	-
84-85	S10	/	-	/	/	-	X
	S11	X	-	/	X	-	X
	S12	O	-	X	X	-	X
	F10	-	-	X	/	-	X
	F11	O	-	/	X	-	X
	F12	X	-	/	X	-	X

LEGEND

' X '= Expected result

' / '= Marginal result

' - '= No significant result

' O '= Results Opposite to expectation

TABLE 3

WINTER 83-84 ACC STATISTICAL SUMMARY

Parameter	Winter Summary	Dec.	Jan.	Feb.
Average Forecast ACC	0.500	.53	.53	.44
Standard Deviation	0.132	.13	.13	.15
Correlation of fcst. and per.	0.155	+.47	-.30	-.20
Number data points	87	31	31	29

TABLE 4

WINTER 84-85 ACC STATISTICAL SUMMARY

Parameter	Winter Summary	Dec.	Jan.	Feb.
Average Forecast ACC	0.490	.46	.50	.52
Standard Deviation	0.171	.18	.16	.17
Correlation of fcst. and per.	0.138	+.26	+.24	-.11
Number data points	82	31	31	23

LIST OF REFERENCES

Bettge, T. W. and D. P. Baumhefner, 1984: Total and Planetary-Scale Systematic Errors in Recent NMC Operational Model Forecasts. Monthly Weather Review, 112, 2371-2325.

Bengtsson, L., and A. J. Simmons, 1983: Medium-range weather prediction - Operational experience at ECMWF. Large Scale Dynamical Processes in the Atmosphere, B.J. Hoskins and R.P. Pearce, Eds., Academic Press, 337-363.

Bengtsson, L., 1985: Medium-Range Forecasting - The Experience of ECMWF. Bulletin of the American Meteorological Society, 79, 1133-1146.

Bettge, T. W., 1983: A Systematic Error Comparison Between the ECMWF and NMC Prediction Models. Bulletin of the American Meteorological Society, 111, 2385-2389.

Boyle, J.S., and C.H. Wash, 1985: Evaluation of NOGAPS 2.1 Systematic Error - Winter 1983/84. Tech. Rep. No. NPS63-85-002, Naval Postgraduate School, 72 pp.

Elsberry, R. T., H. D. Hamilton, and P. A. Petit, 1985: Accuracy and Operational Use of Medium and Extended range Numerical Atmospheric Forecasts: A Review. Naval Environmental Prediction Research Facility Contractor Report CR 85-02, 84 pp.

Gronaas, S., 1982: Systematic Errors and Forecast Quality of ECMWF Forecasts in Different Large-Scale Flow Patterns. ECMWF Seminar/Workshop 1982, 161-202.

Haltiner, G.J. and R.T. Williams, 1980: Numerical Prediction and Dynamic Meteorology (Second Edition). John Wiley and Sons, 477 pp.

Hollingsworth, A., K. Arpe, M. Tiedtke, M. Capaldo, and H. Savijarvi, 1980: The performance of a medium-range forecast model in winter - Impact of physical parameterizations. Monthly Weather Review, 108, 1736-1773.

IMSL, 1982, Library Reference manual, Edition 9, Volume 2, F-1 to F-6. IMSL Inc., Huston, Texas 77036-5085.

Miyakoda, K., G. D. Hembree, R. F. Strickler, and I. Shulman, 1972: Cumulative results of extended forecast experiments. Part 1: Model performance for winter cases. Monthly Weather Review, 100, 836-855.

Nieminen, R., 1983: Operational verification of ECMWF forecast fields and results for 1980-81. Tech. Rep. No. 36, ECMWF, 47 pp.

Quiroz, R. S., 1984: The Climate of the 1983-84 Winter - A Season of Strong Blocking and Severe Cold in North America. Monthly Weather Review, 112, 1894-1912.

Wallace, J. M., and J. K. Woessner, 1981: An Analysis of Forecast Error in the NMC Primitive Equation Model. Monthly Weather Review, 109 2444-2449.

INITIAL DISTRIBUTION LIST

		No. Copies
1.	Defense Technical Information Center Cameron Station Alexandria, VA 22304-6145	2
2.	Library, Code 0142 Naval Postgraduate School Monterey, CA 93943	2
3.	Chairman (Code 63Rd) Department of Meteorology Naval Postgraduate School Monterey, CA 93943	1
4.	Chairman (Code 68Mr) Department of Oceanography Naval Postgraduate School Monterey, CA 93943	1
5.	Professor C. Wash (Code 63Wa) Department of Meteorology Naval Postgraduate School Monterey, CA 93943	10
6.	Professor J. Boyle (Code 63Bo) Department of Meteorology Naval Postgraduate School Monterey, CA 93943	1
7.	LT John E. Curtis USS New Orleans (LPH-11) FPO San Francisco, CA 96627-1650	1
8.	Director Naval Oceanography Division Naval Observatory 34th and Massachusetts Avenue NW Washington, DC 20390	1
9.	Commander Naval Oceanography Command NSTL Station Bay St. Louis, MS 39522	1
10.	Commanding Officer Naval Oceanographic Office NSTL Station Bay St. Louis, MS 39522	1
11.	Commanding Officer Fleet Numerical Oceanography Center Monterey, CA 93940	1
12.	Commanding Officer Naval Ocean Research and Development Activity NSTL Station Bay St. Louis, MS 39522	1
13.	Commanding Officer Naval Environmental Prediction Research Facility Monterey, CA 93940	1

14. Chairman, Oceanography Department 1
U.S. Naval Academy
Annapolis, MD 21402

15. Chief of Naval Research 1
800 N. Quincy Street
Arlington, VA 22217

16. Office of Naval Research (Code 420) 1
Naval Ocean Research and Development Activity
800 N. Quincy Street
Arlington, VA 22217

17. Scientific Liaison Office 1
Office of Naval Research
Scripps Institution of Oceanography
La Jolla, CA 92037

18. Library 1
Scripps Institution of Oceanography
P.O. Box 2367
La Jolla, CA 92037

19. Library 1
Department of Oceanography
University of Washington
Seattle, WA 98105

20. Library 1
CICESE
P.O. Box 4803
San Ysidro, CA 92073

21. Library 1
School of Oceanography
Oregon State University
Corvallis, OR 97331

23. Commander 1
Oceanographic Systems Pacific
Box 1390
Pearl Harbor, HI 96860

24. Commanding Officer 1
Naval Eastern Oceanography Center
Naval Air Station
Norfolk, VA 23511

25. Commanding Officer 1
Naval Western Oceanography Center
Box 113
Pearl Harbor, HI 96860

26. Commanding Officer 1
Naval Oceanography Command Center, Rota
Box 31
FPO San Francisco, CA 09540

27. Commanding Officer 1
Naval Oceanography Command Center, Guam
Box 12
FPO San Francisco, CA 96630

END

FILMED

3-86

DTIC